Electronic Supplementary Material (ESI) for Dalton Transactions.

Experimental Determination of Redox Cooperativity and Electronic Structure in Catalytically Active Cu-Fe and Zn-Fe Heterobimetallic Complexes

Malkanthi K. Karunananda, Francisco X. Vázquez, E. Ercan Alp, Wenli Bi, Soma Chattopadhyay, Tomohiro Shibata, Neal P. Mankad

Supporting Information

Table of Contents

Figure S19: Cu K-edge spectrum for (IMes)CuCl

Figure S20: Cu K-edge spectrum for (IPr)CuI

Figure S21: Cu K-edge spectrum for (IPr)CuFp

Figure S22: Cu K-edge spectrum for (IMes)CuFp

Figure S23: Cu K-edge spectrum for (IPr)CuMp

Figure S24: Zn K-edge spectrum for Zn foil

Figure S25: Zn K-edge spectrum for $ZnCl_2$

Figure S26: Zn K-edge spectrum for (IPr)$ZnCl_2$.THF

Figure S27: Zn K-edge spectrum for (IPr)(Cl)ZnFp

Figure S28 : Fe K-edge : Plot of 1st derivate of normalized intensity for Fe foil

Figure S29 : Fe K-edge : Plot of 1st derivate of normalized intensity for for $FeCl_2$

Figure S30 : Fe K-edge : Plot of 1st derivate of normalized intensity for for $FeCl_3$

Figure S31 : Fe K-edge : Plot of 1st derivate of normalized intensity for for K^+Fp^-

Figure S32 : Fe K-edge : Plot of 1st derivate of normalized intensity for for FpI

Figure S33 : Fe K-edge : Plot of 1st derivate of normalized intensity for for FpMe

Figure S34 : Fe K-edge : Plot of 1st derivate of normalized intensity for for (IPr)CuFp

Figure S35 : Fe K-edge : Plot of 1st derivate of normalized intensity for for (IMes)CuFp

Figure S36 : Fe K-edge : Plot of 1st derivate of normalized intensity for for (IPr)(Cl)ZnFp

Figure S37 : Fe K-edge : Plot of 1st derivate of normalized intensity for for Fp_2

Figure S38: Zn K-edge : Plot of 1st derivate of normalized intensity for for Zn foil

Figure S39: Zn K-edge : Plot of 1st derivate of normalized intensity for for $ZnCl_2$

Figure S40: Zn K-edge : Plot of 1st derivate of normalized intensity for for (IPr)$ZnCl_2$.THF

Figure S41: Zn K-edge : Plot of 1st derivate of normalized intensity for for (IPr)(Cl)ZnFp

Figure S42: Fe K-edge air oxidation monitoring of bimetallic complexes containing Fe and comparison with Fp_2 dimer: Fe K-edge spectra of the Fp_2 dimer (red) & (IPr)CuFp before oxidation (green) and after oxidation (blue). The spectra of (IMes)CuFp & (IPr)(Cl)ZnFp after oxidation also matched the spectrum of the Fp_2 dimer

Figure S43: Cu K-edge air oxidation monitoring of (IPr)CuFp: Cu K-edge spectra of (IPr)CuFp before oxidation (red) and after oxidation (blue)

Figure S65: Deconvoluted Cu K-edge spectrum for (IPr)CuMp

Figure S66: Deconvoluted Cu K-edge spectrum for (IMes)CuCl

Figure S67: Deconvoluted Cu K-edge spectrum for (IPr)CuI

Figure S68: Deconvoluted Cu K-edge spectrum for (IPr)CuCl

Table S2: Deconvolution parameters used for XAS spectra analysis using Athena software

Figure S69: IR Spectrum of Fp_2

Figure S70: IR Spectrum of K^+Fp^-

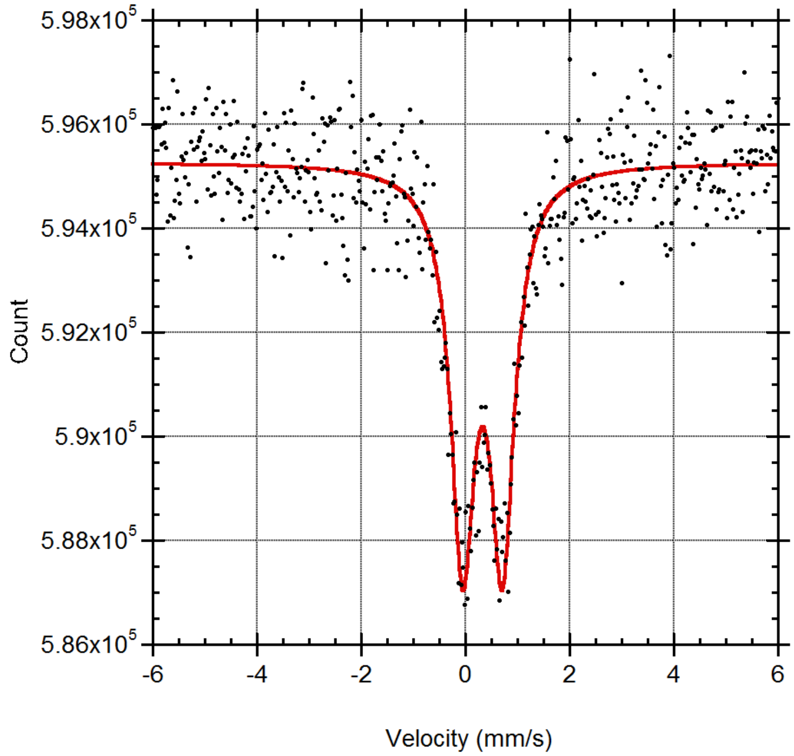

Figure S1: Mössbauer data (black) and fit (red) for (IMes)CuFp

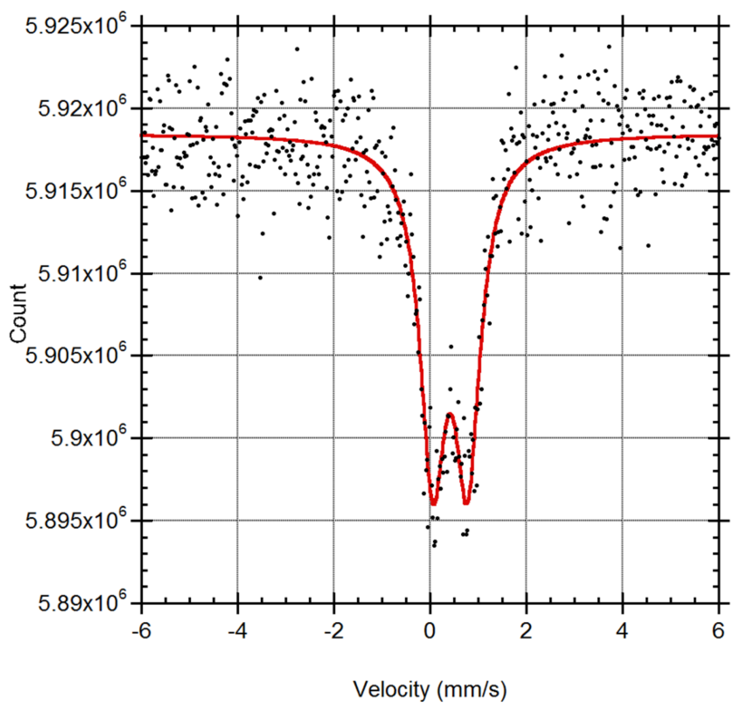

Figure S2: Mössbauer data (black) and fit (red) for (IPr)(Cl)ZnFp

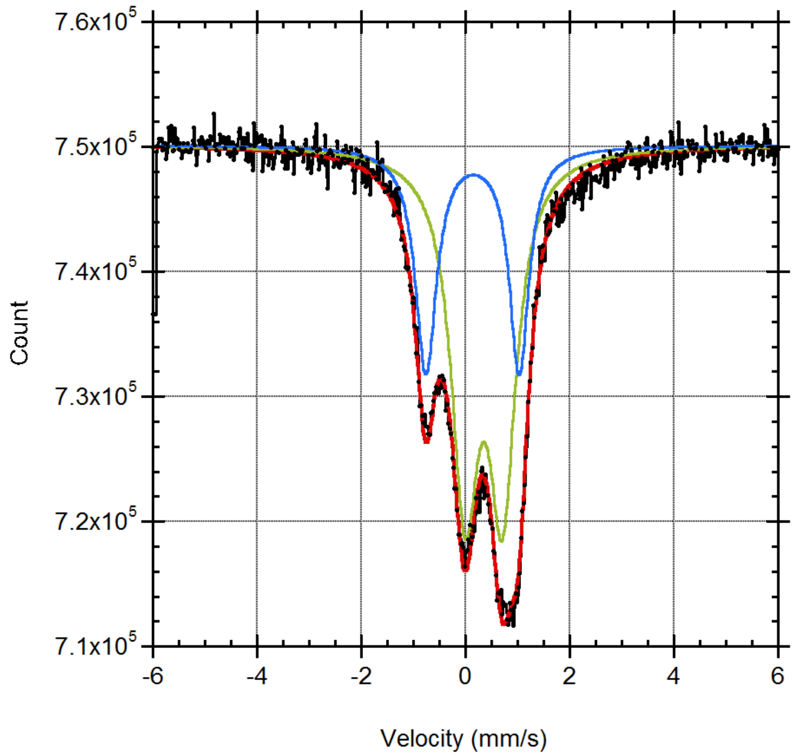

Figure S3: Mössbauer data (black), fit (red), site 1(blue) and site 2 (green) for $K^{+}Fp^{-}$

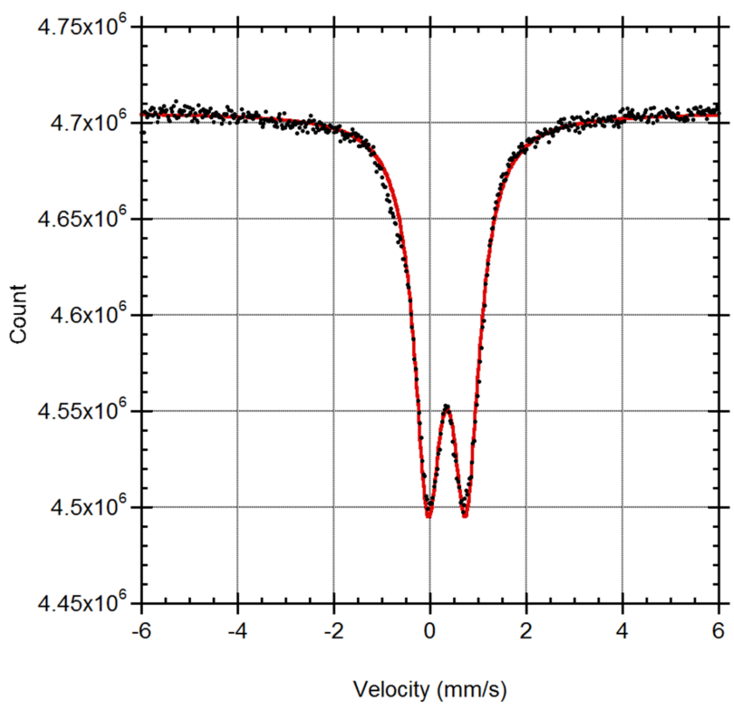

Figure S4: Mössbauer data (black) and fit (red) for $[K(18\text{-crown-}6)_2][Fp]$

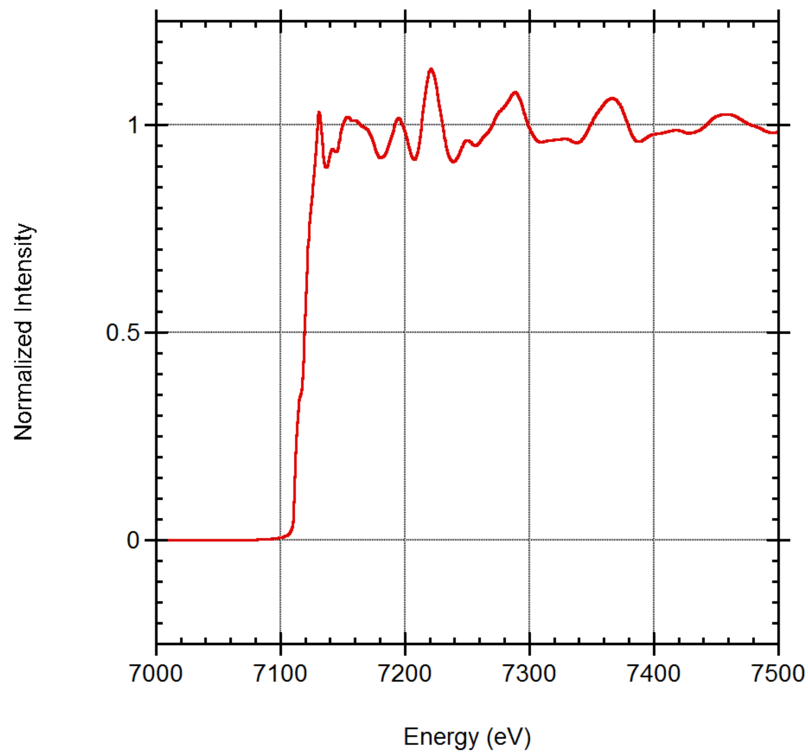

Figure S5 : Fe K-edge spectrum for Fe foil

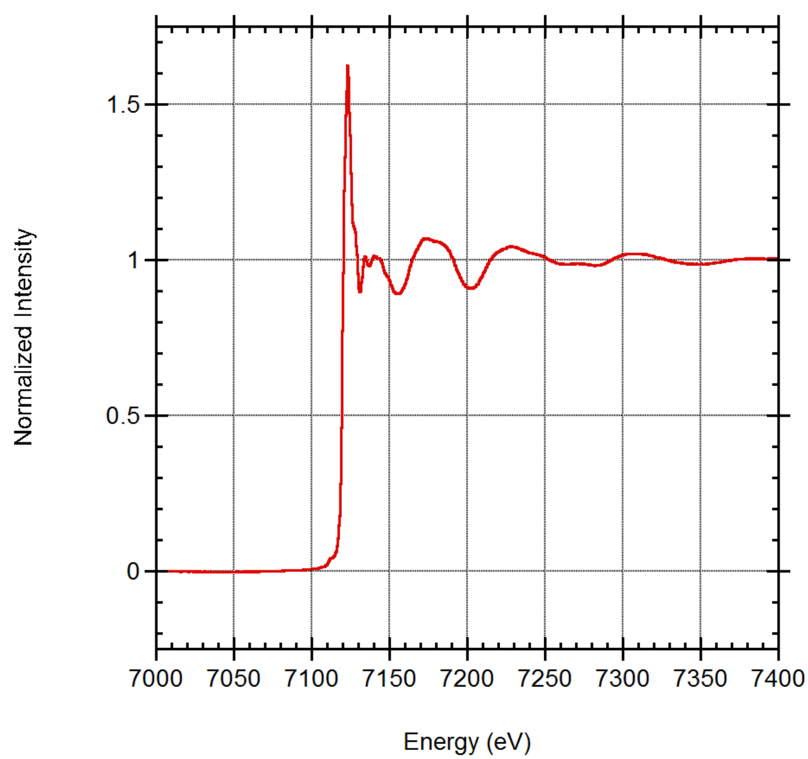

Figure S6 : Fe K-edge spectrum for $FeCl_2$

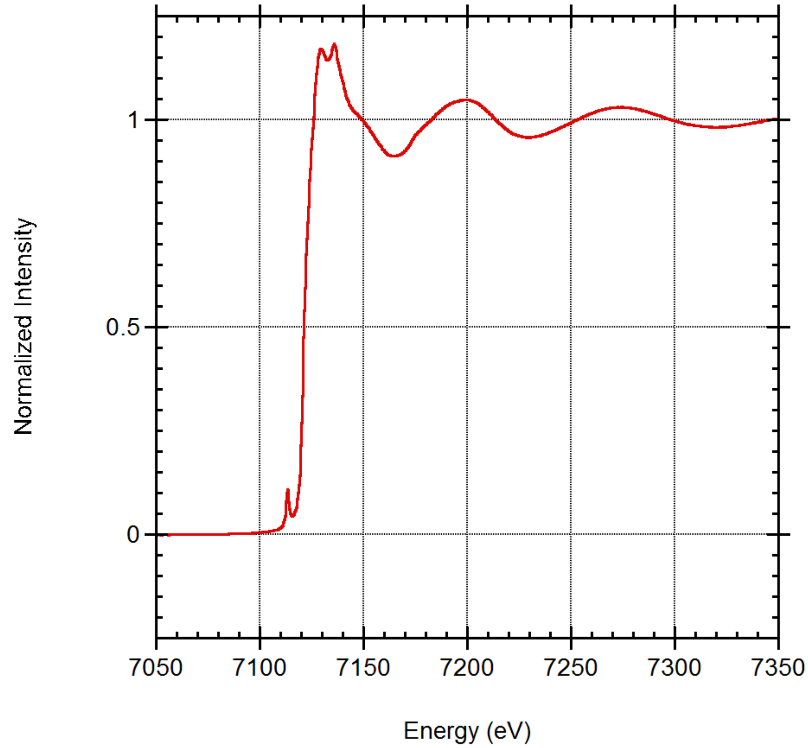

Figure S7 : Fe K-edge spectrum for $FeCl_3$

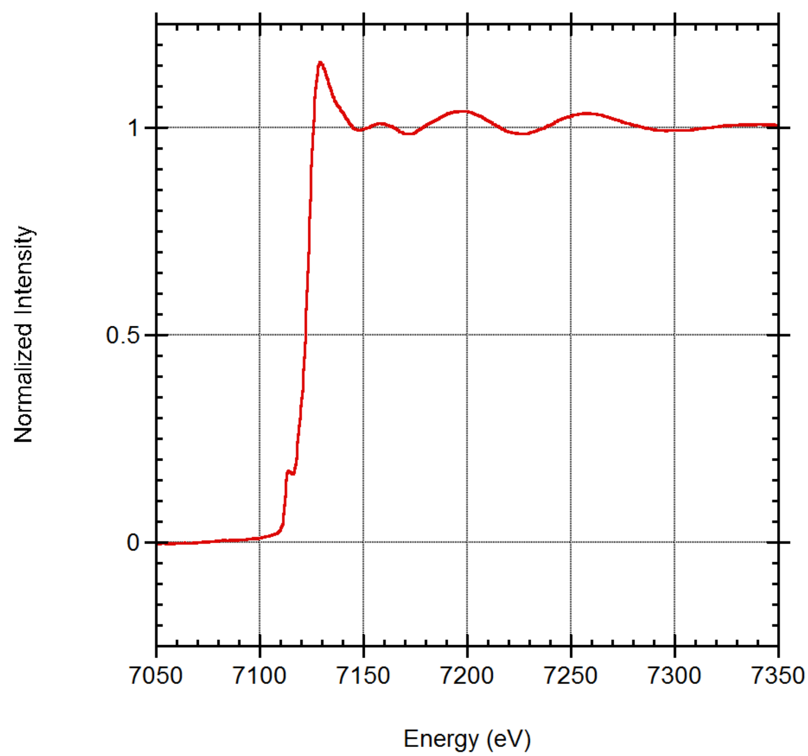

Figure S8 : Fe K-edge spectrum for K^+Fp^-

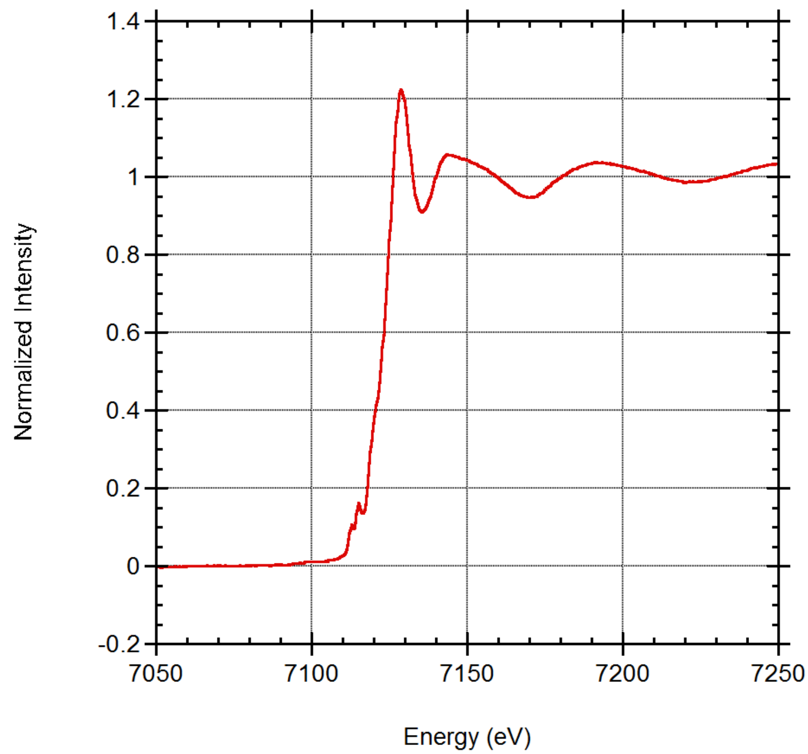

Figure S9 : Fe K-edge spectrum for FpI

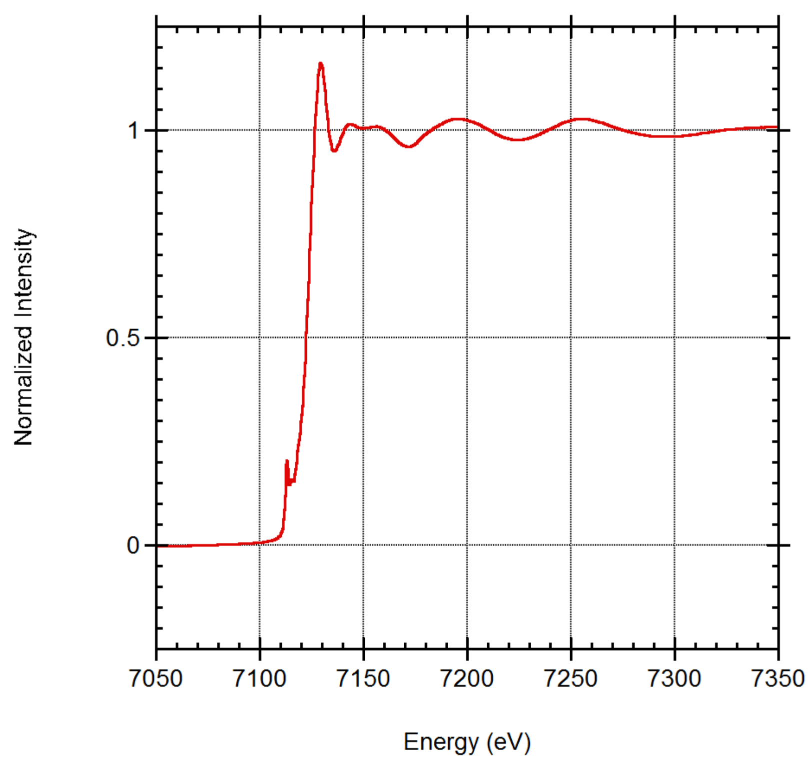

Figure S10 : Fe K-edge spectrum for FpMe

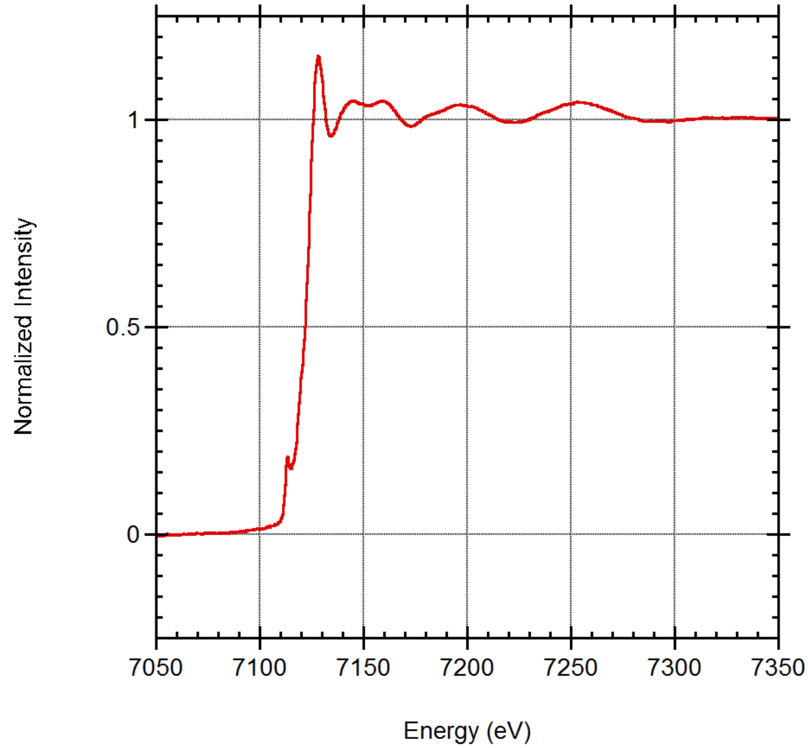

Figure S11 : Fe K-edge spectrum for (IPr)CuFp

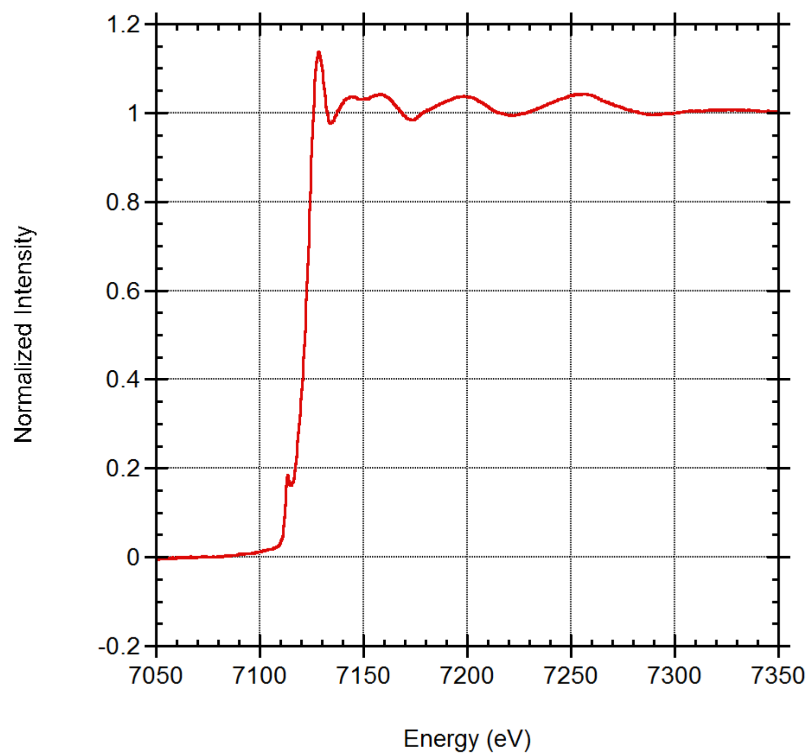

Figure S12 : Fe K-edge spectrum for (IMes)CuFp

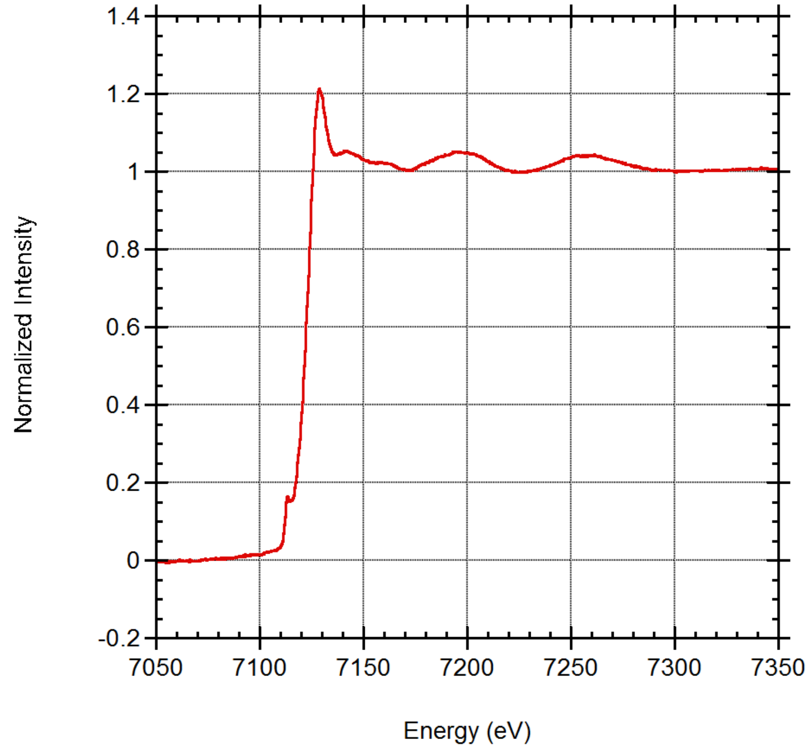

Figure S13 : Fe K-edge spectrum for (IPr)(Cl)ZnFp

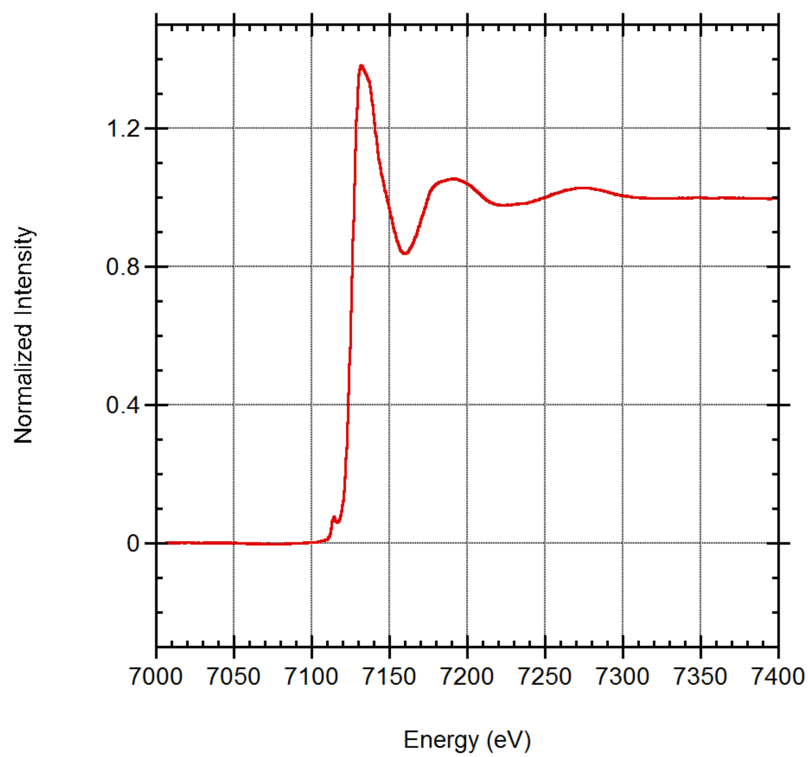

Figure S14 : Fe K-edge spectrum for Fp_2

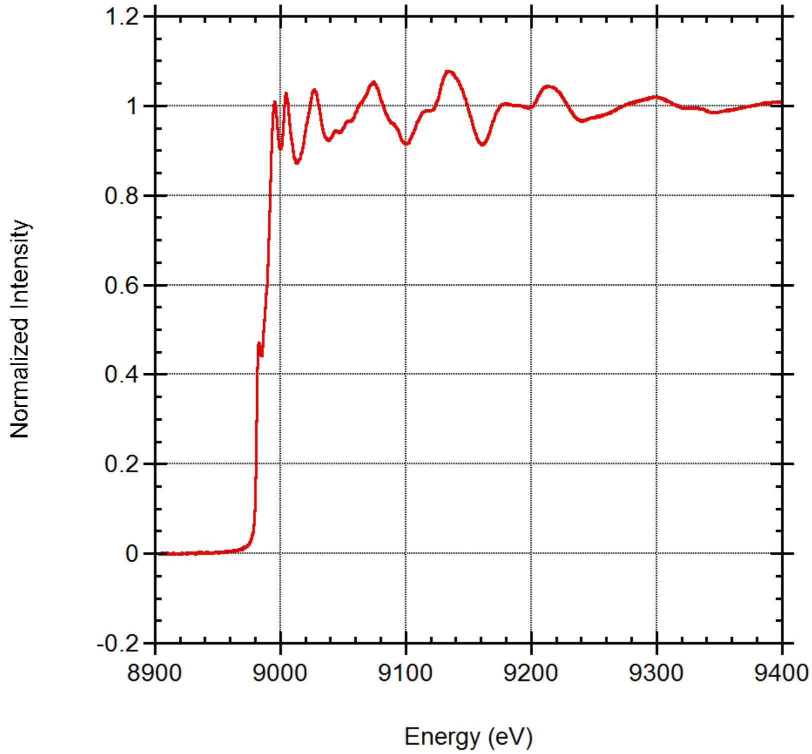

Figure S15: Cu K-edge spectrum for Cu foil

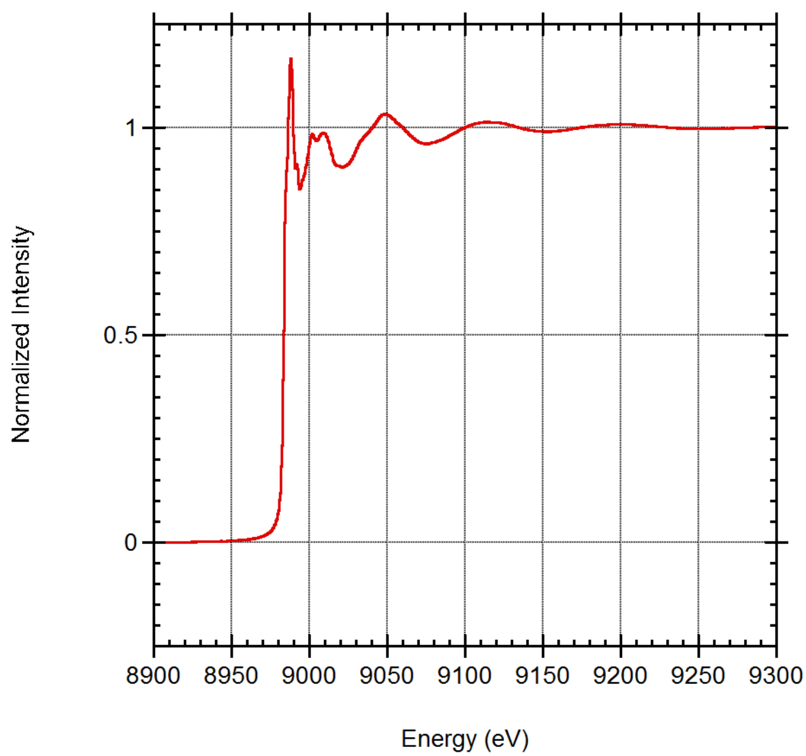

Figure S16: Cu K-edge spectrum for CuCl

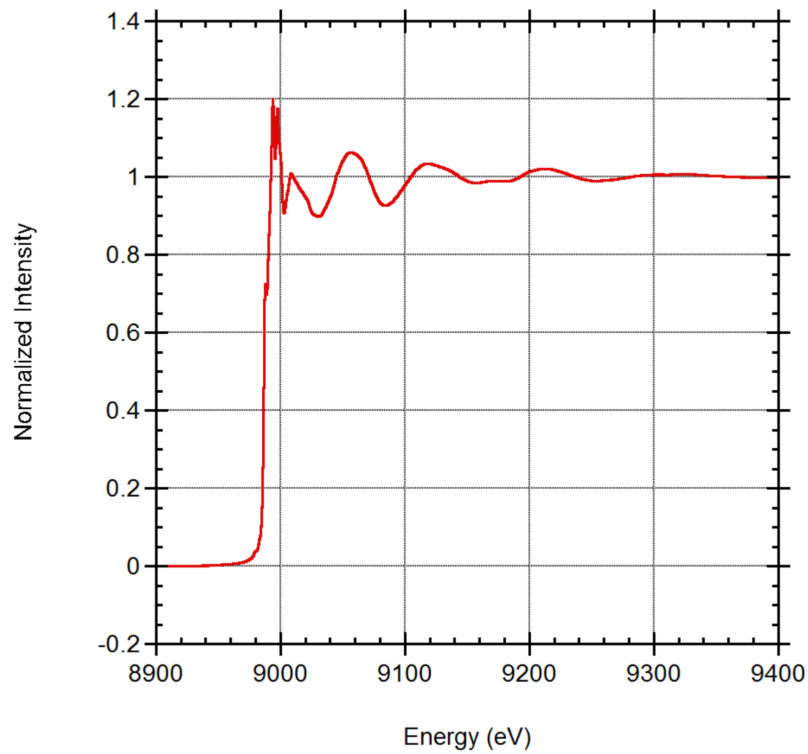

Figure S17: Cu K-edge spectrum for $CuCl_2$

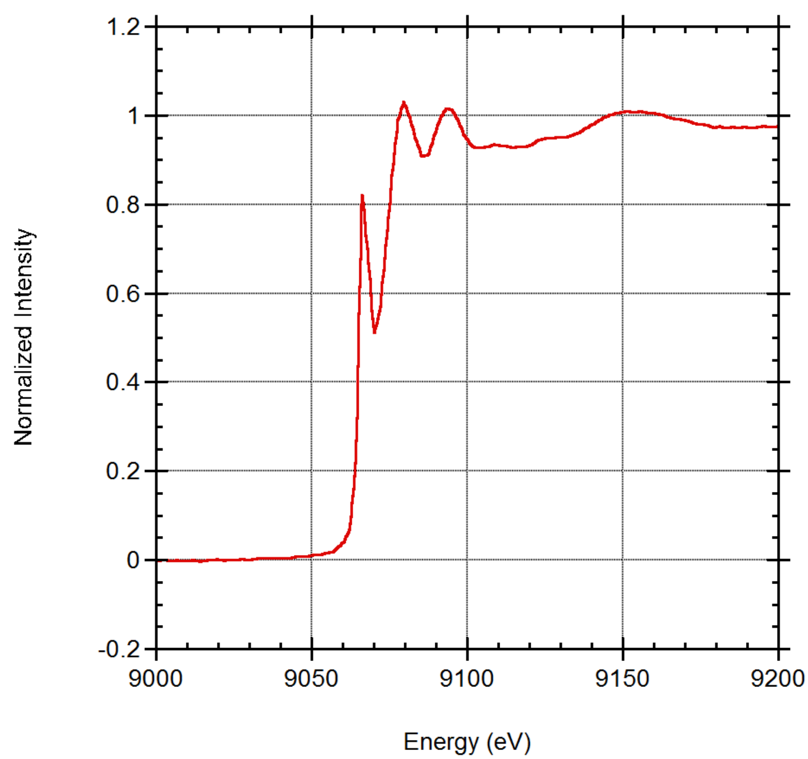

Figure S18: Cu K-edge spectrum for (IPr)CuCl

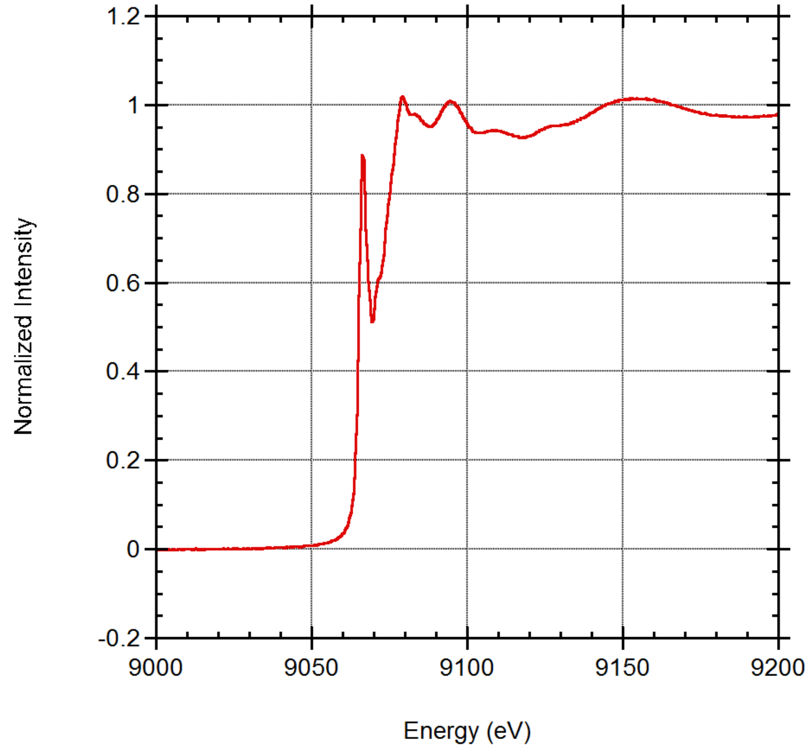

Figure S19: Cu K-edge spectrum for (IMes)CuCl

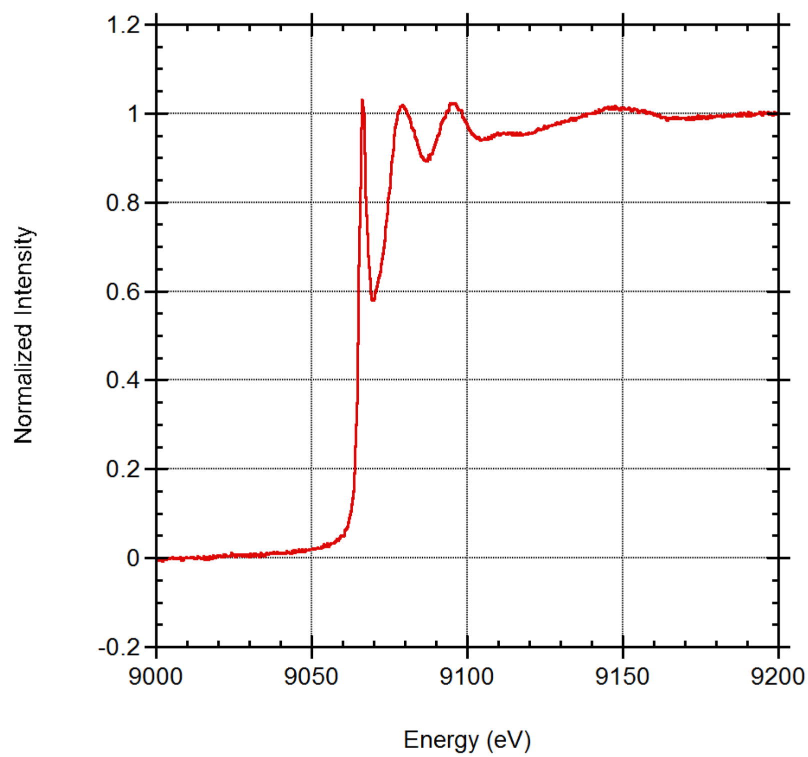

Figure S20: Cu K-edge spectrum for (IPr)CuI

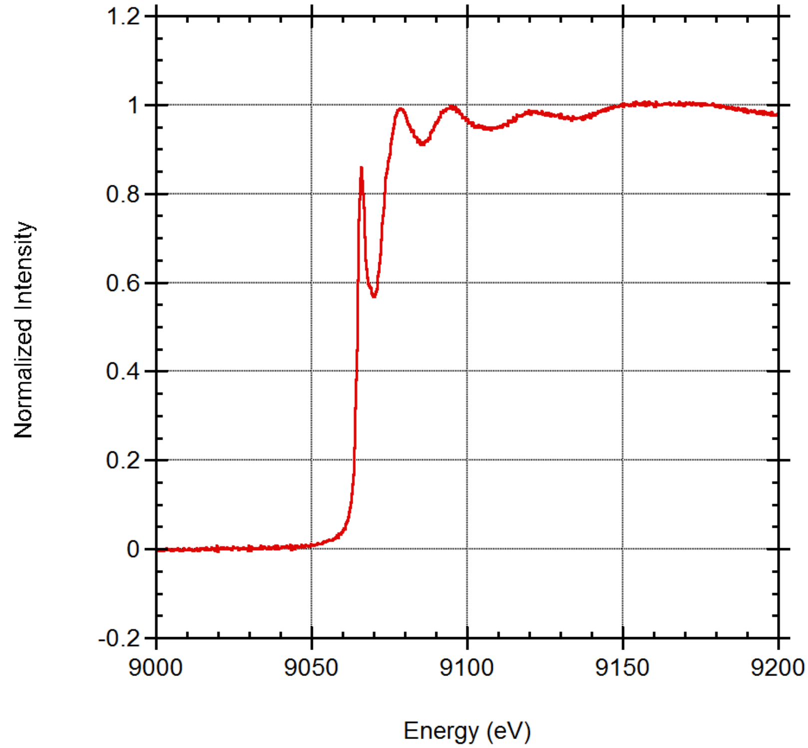

Figure S21: Cu K-edge spectrum for (IPr)CuFp

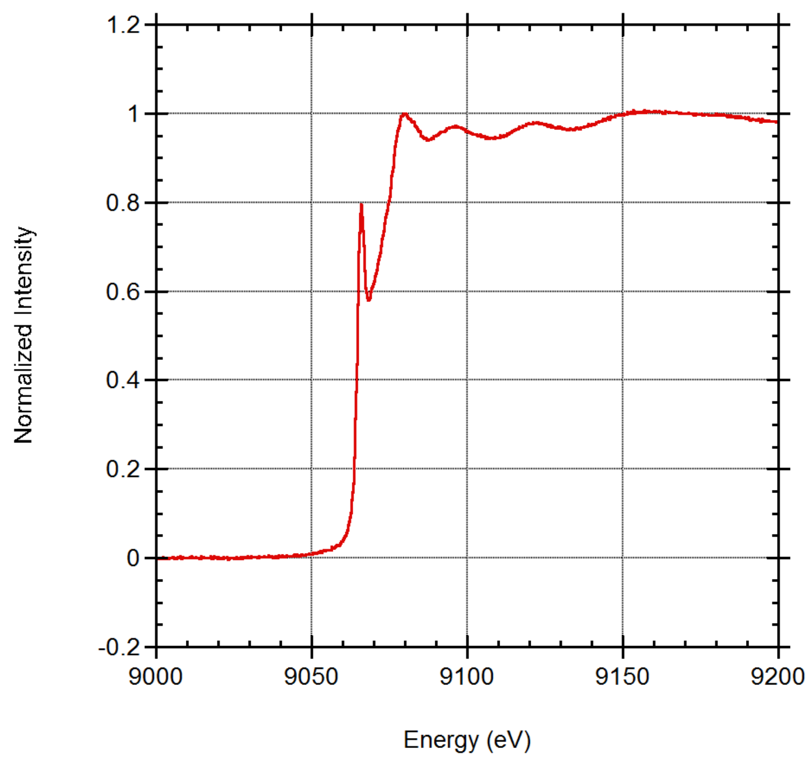

Figure S22: Cu K-edge spectrum for (IMes)CuFp

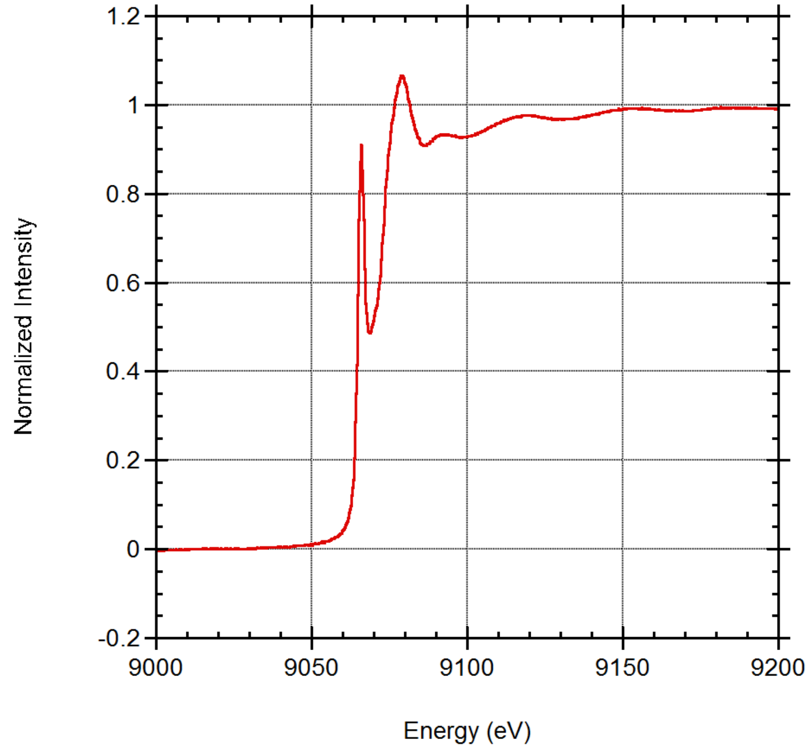

Figure S23: Cu K-edge spectrum for (IPr)CuMp

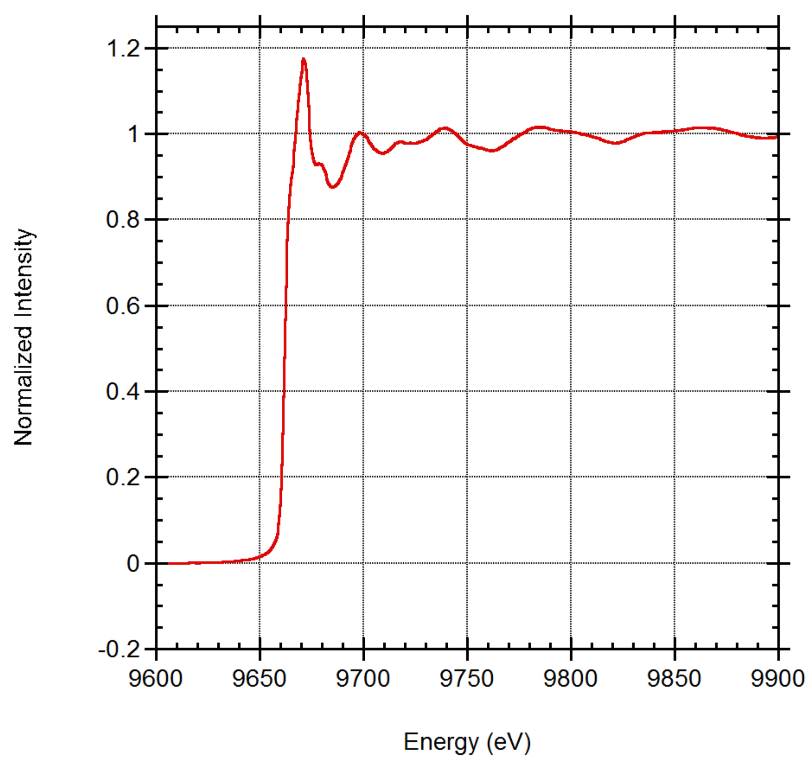

Figure S24: Zn K-edge spectrum for Zn foil

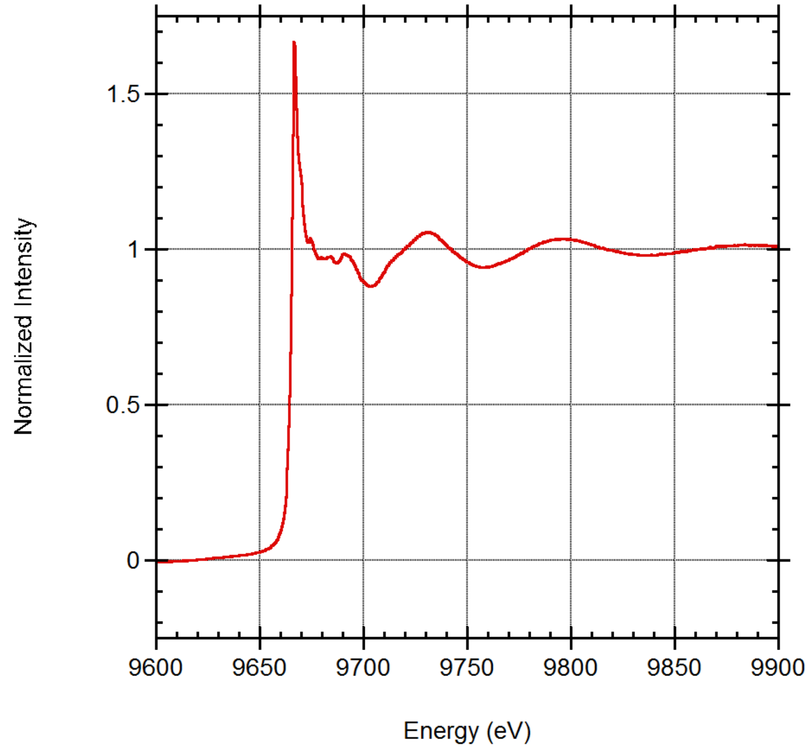

Figure S25: Zn K-edge spectrum for $ZnCl_2$

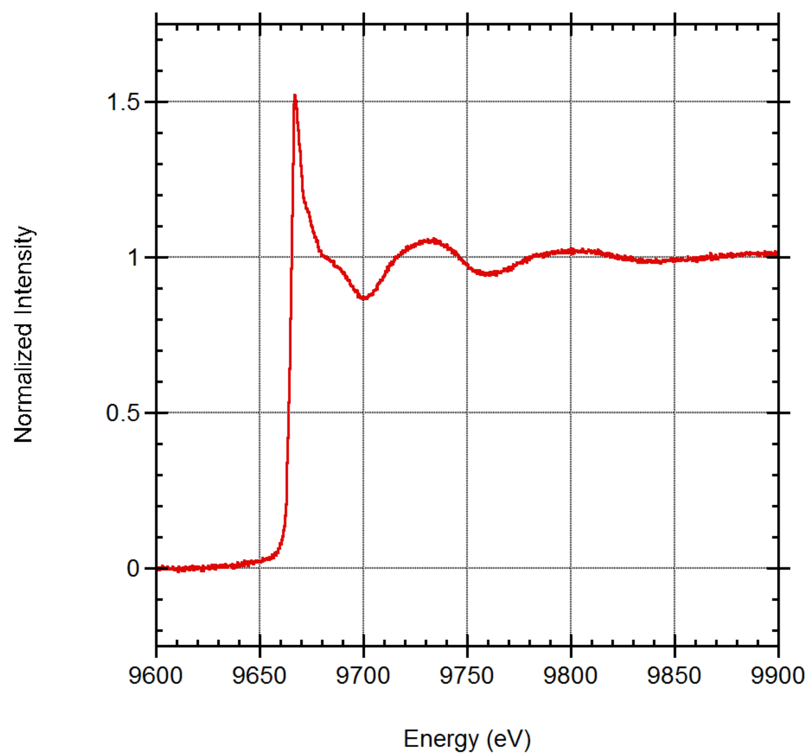

Figure S26: Zn K-edge spectrum for (IPr)$ZnCl_2$.THF

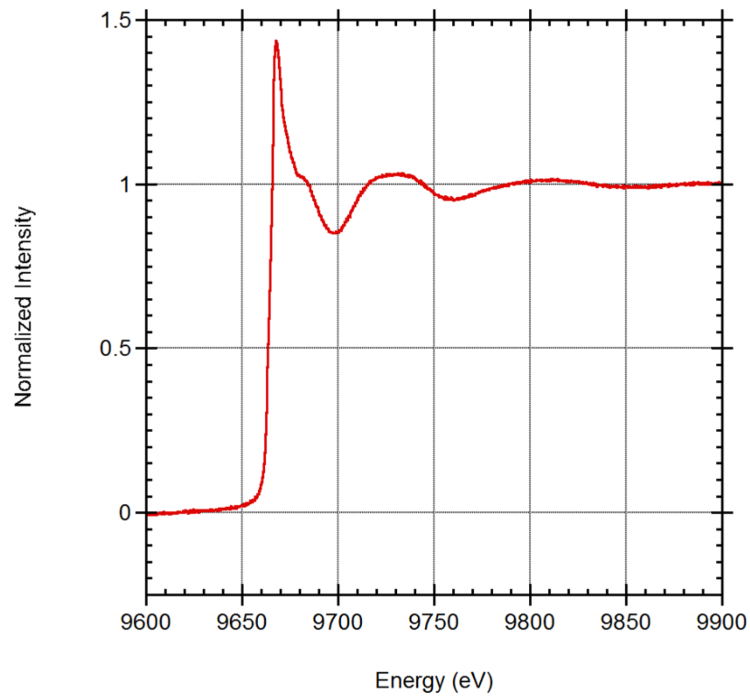

Figure S27: Zn K-edge spectrum for (IPr)(Cl)ZnFp

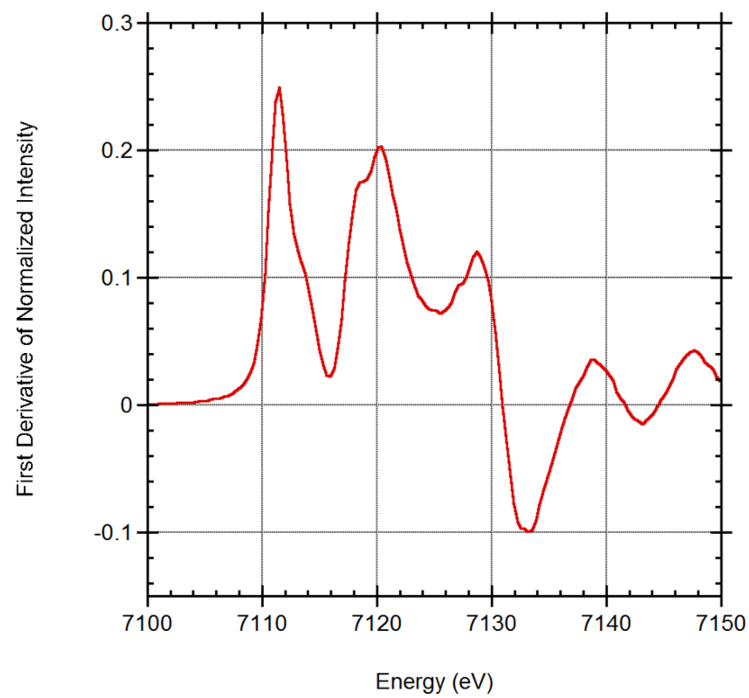

Figure S28 : Fe K-edge : Plot of 1st derivate of normalized intensity for Fe foil

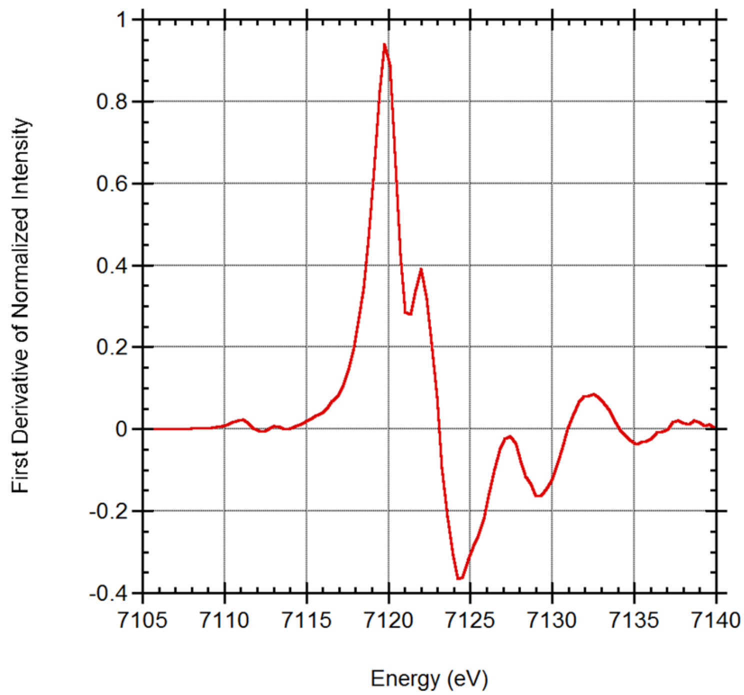

Figure S29 : Fe K-edge : Plot of 1st derivate of normalized intensity for for $FeCl_2$

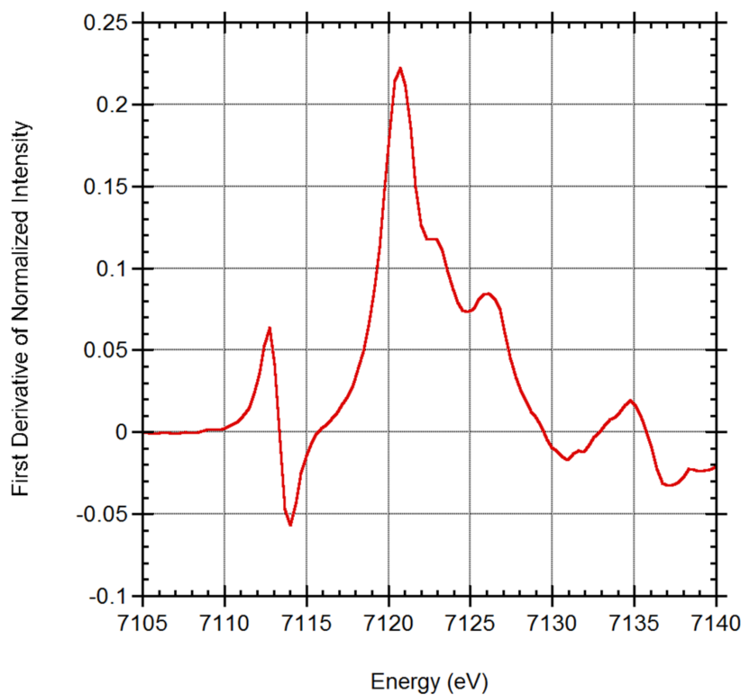

Figure S30 : Fe K-edge : Plot of 1st derivate of normalized intensity for for $FeCl_3$

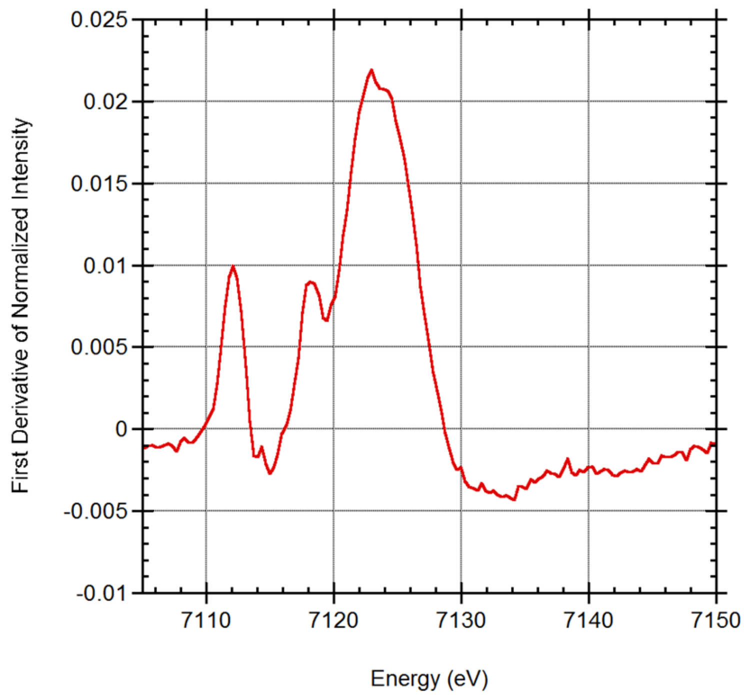

Figure S31 : Fe K-edge : Plot of 1st derivate of normalized intensity for for K^+Fp^-

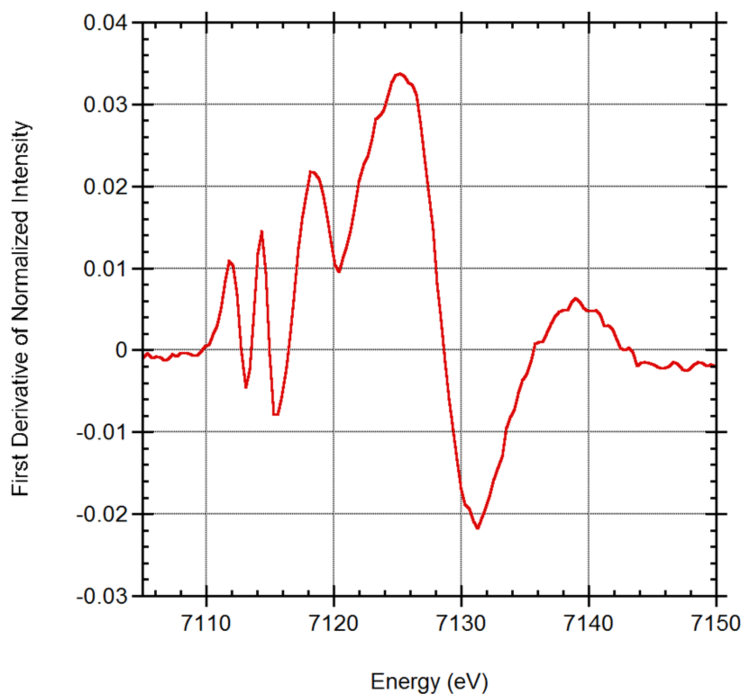

Figure S32 : Fe K-edge : Plot of 1st derivate of normalized intensity for for FpI

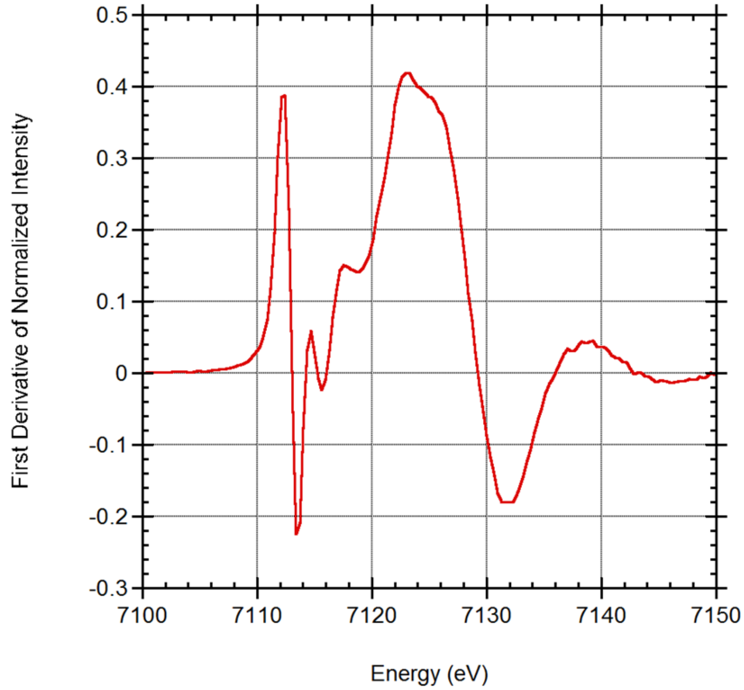

Figure S33 : Fe K-edge : Plot of 1st derivate of normalized intensity for for FpMe

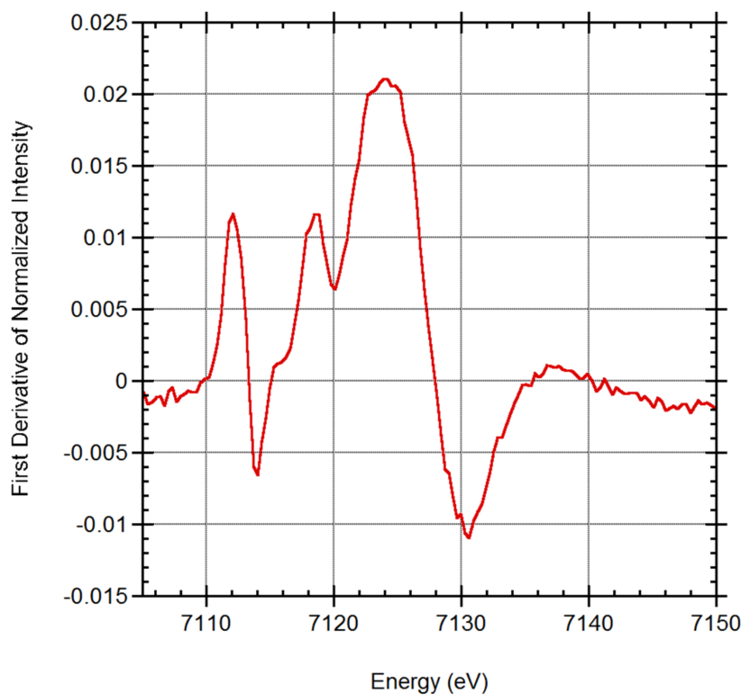

Figure S34 : Fe K-edge : Plot of 1st derivate of normalized intensity for for (IPr)CuFp

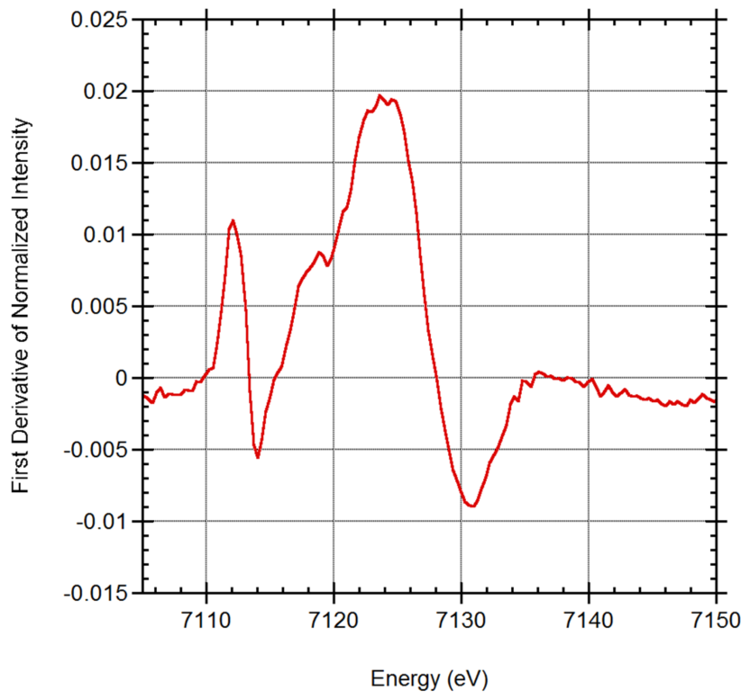

Figure S35 : Fe K-edge : Plot of 1st derivate of normalized intensity for for (IMes)CuFp

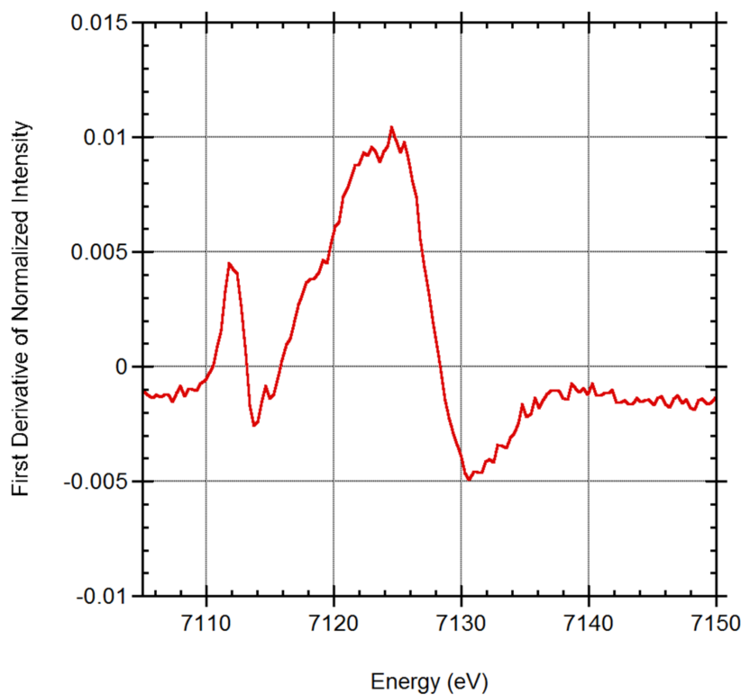

Figure S36 : Fe K-edge : Plot of 1st derivate of normalized intensity for for (IPr)(Cl)ZnFp

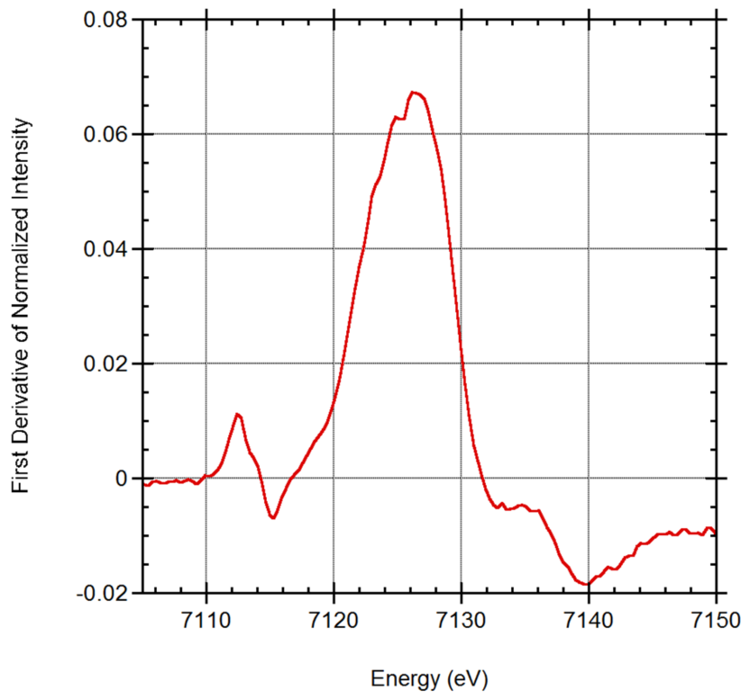

Figure S37 : Fe K-edge : Plot of 1st derivate of normalized intensity for for Fp_2

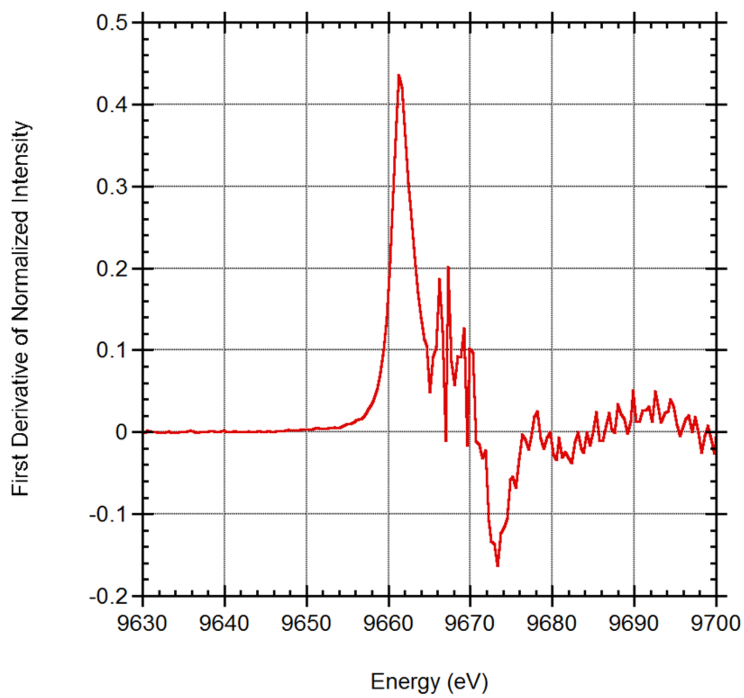

Figure S38: Zn K-edge : Plot of 1st derivate of normalized intensity for for Zn foil

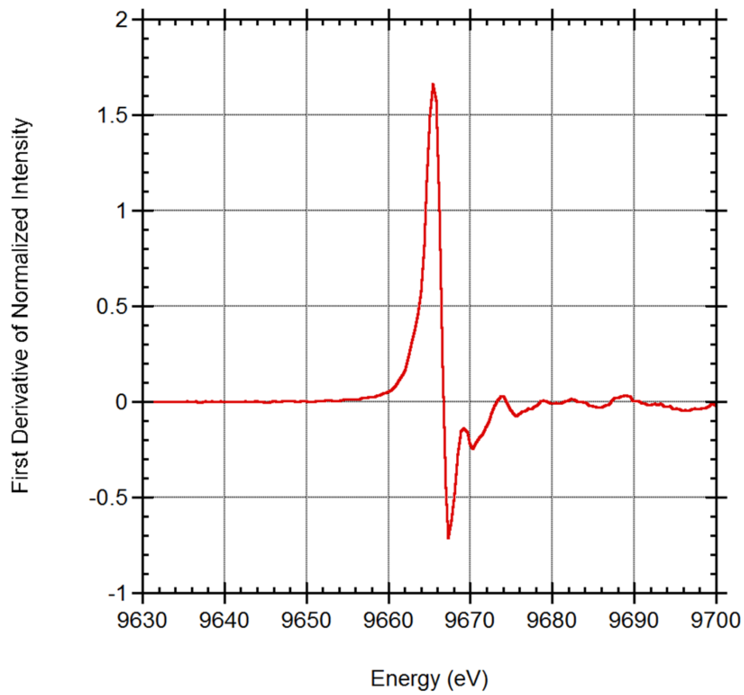

Figure S39: Zn K-edge : Plot of 1st derivate of normalized intensity for for $ZnCl_2$

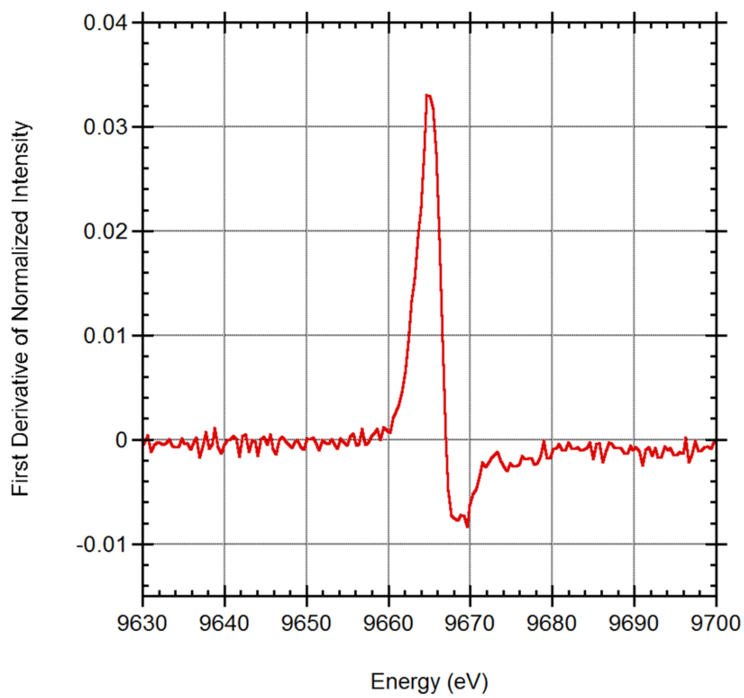

Figure S40: Zn K-edge : Plot of 1st derivate of normalized intensity for for (IPr)$ZnCl_2$.THF

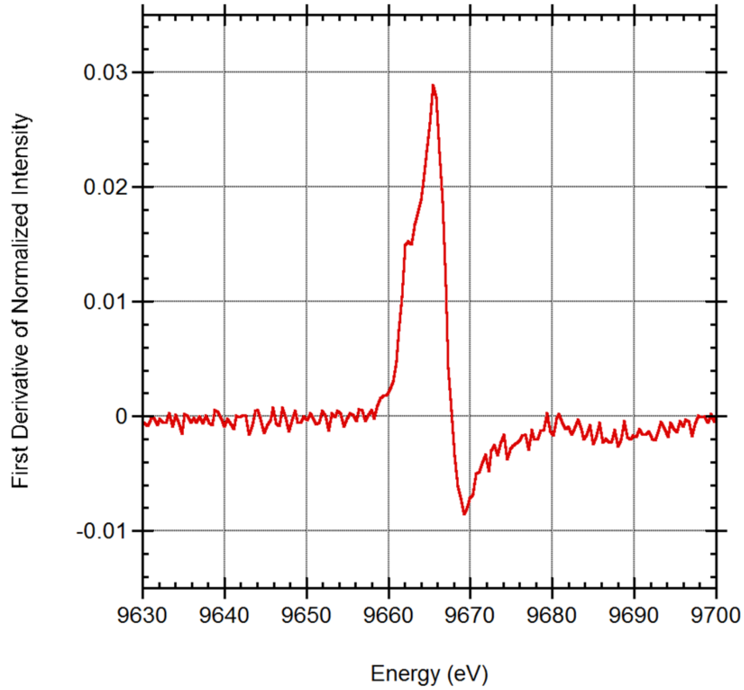

Figure S41: Zn K-edge : Plot of 1st derivate of normalized intensity for for (IPr)(Cl)ZnFp

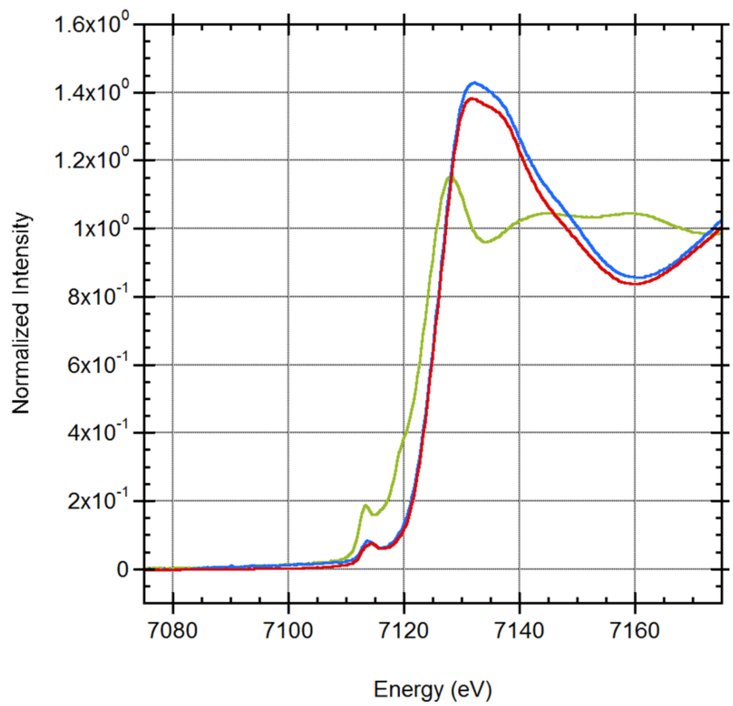

Figure S42: Fe K-edge air oxidation monitoring of bimetallic complexes containing Fe and comparison with Fp_2 dimer: Fe K-edge spectra of the Fp_2 dimer (red) & (IPr)CuFp before oxidation (green) and after oxidation (blue). The spectra of (IMes)CuFp & (IPr)(Cl)ZnFp after oxidation also matched the spectrum of the Fp_2 dimer

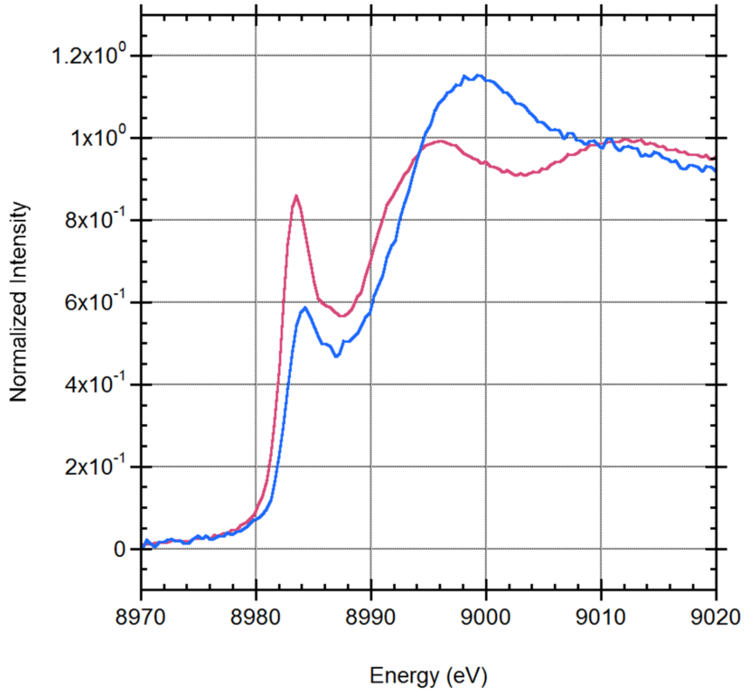

Figure S43: Cu K-edge air oxidation monitoring of (IPr)CuFp: Cu K-edge spectra of (IPr)CuFp before oxidation (red) and after oxidation (blue)

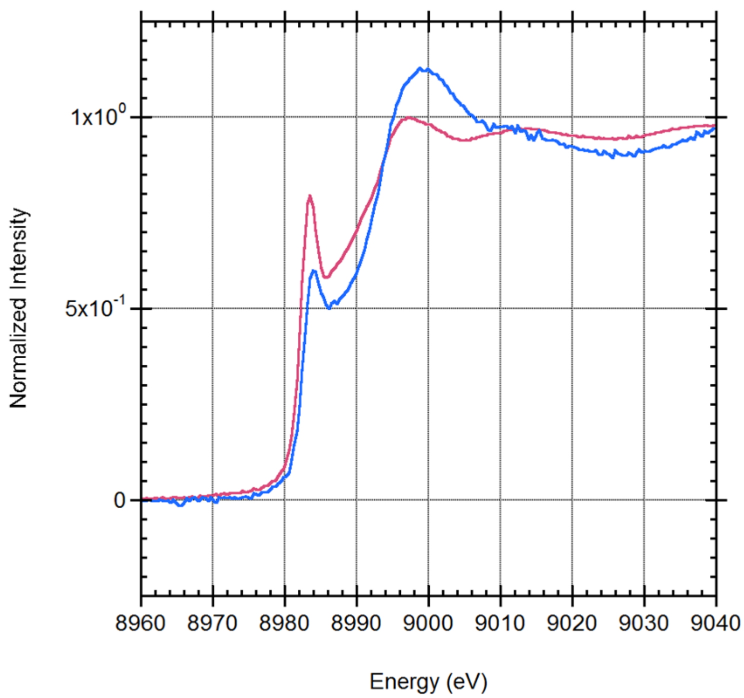

Figure S44: Cu K-edge air oxidation monitoring of (IMes)CuFp: Cu K-edge spectra of (IMes)CuFp before oxidation (red) and after oxidation (blue)

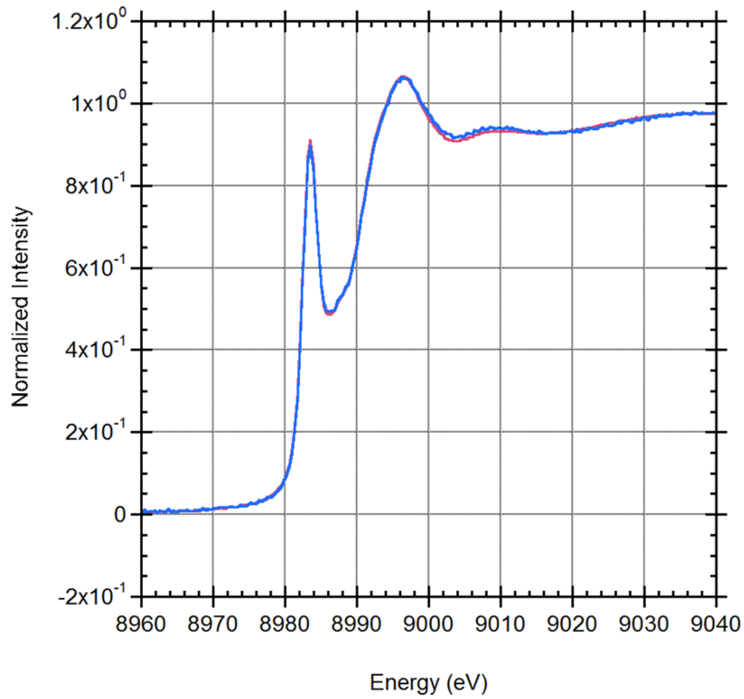

Figure S45: Cu K-edge air oxidation monitoring of (IPr)CuMp: Cu K-edge spectra of (IPr)CuMp before oxidation (red) and after oxidation (blue)

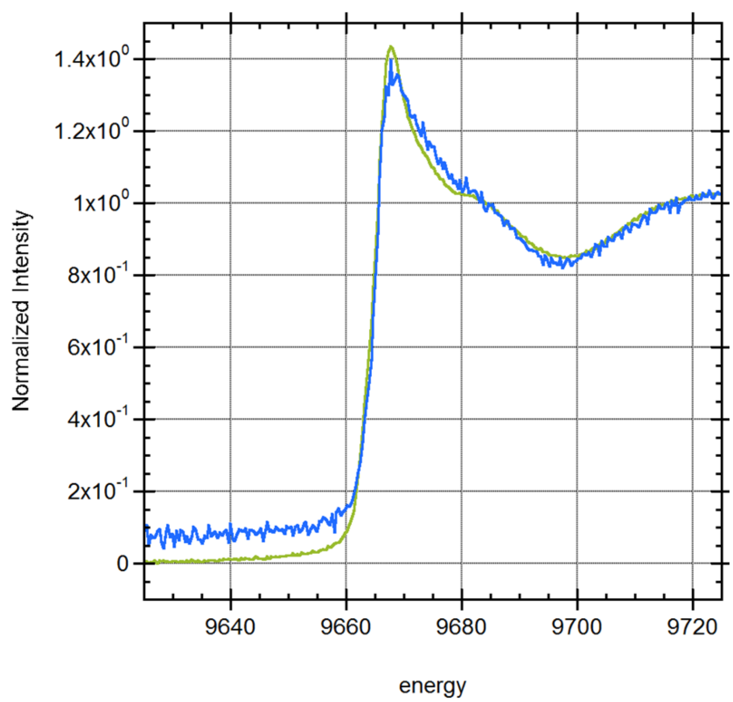

Figure S46: Zn K-edge air oxidation monitoring of (IPr)(Cl)ZnFp: Zn K-edge spectra of (IPr)(Cl)ZnFp before oxidation (green) and after oxidation (blue)

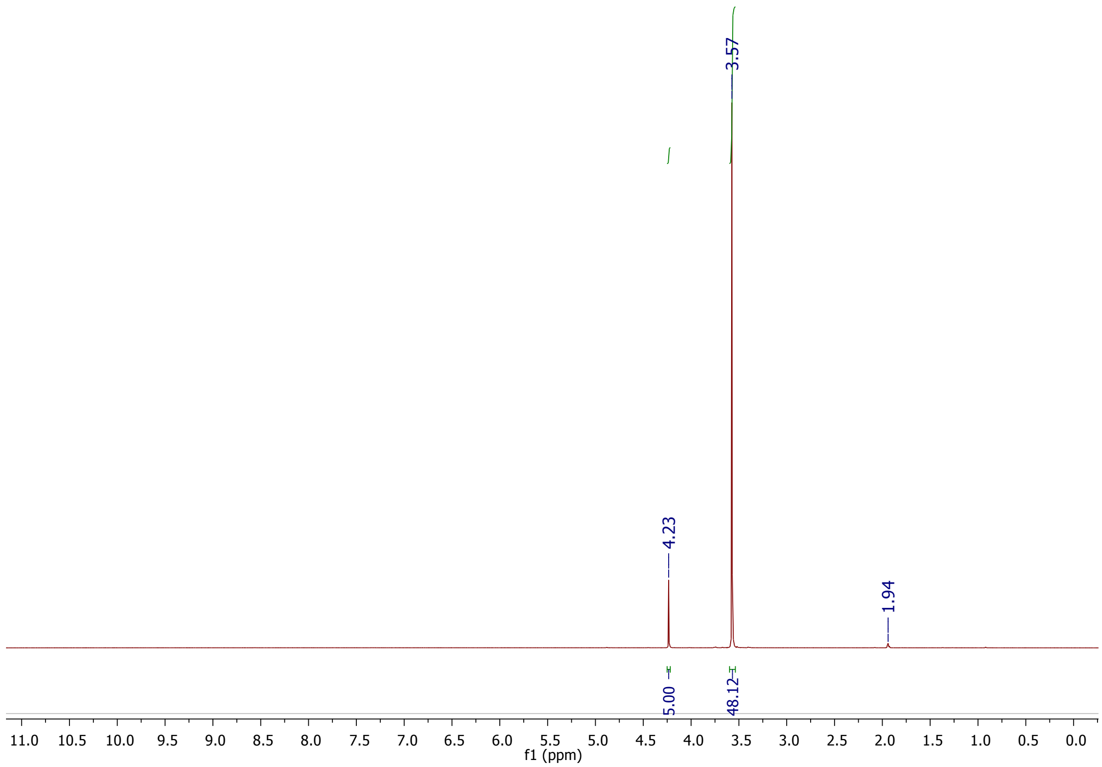

Figure S47: H^1 NMR of $[K(18\text{-crown-}6)_2][Fp]$ in CD_3CN (400 MHz)

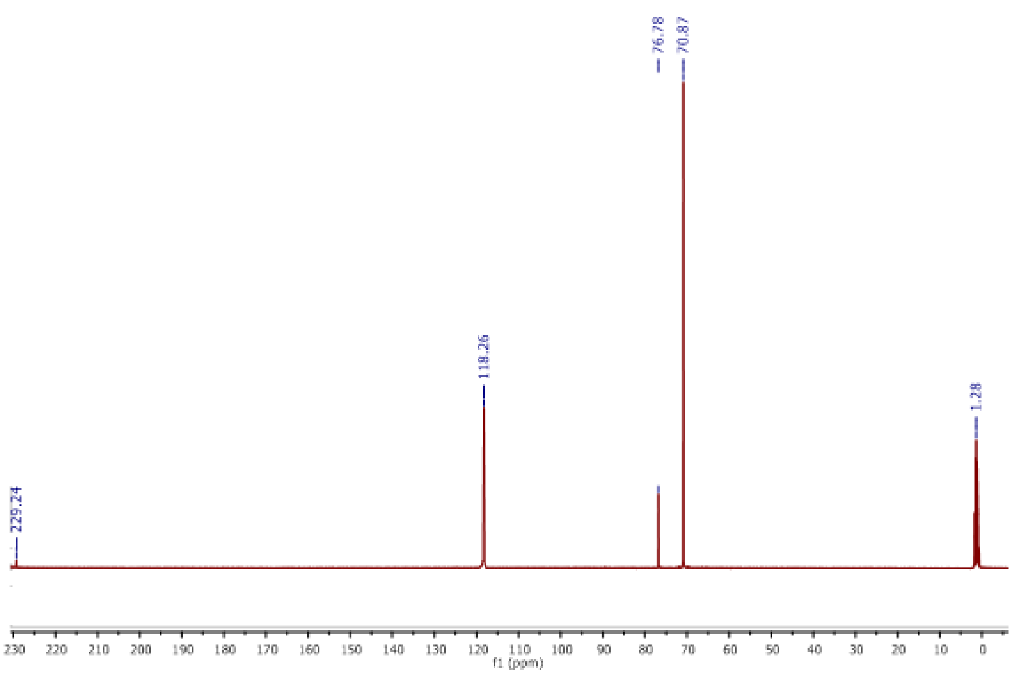

Figure S48: C^{13} NMR of $[K(18\text{-crown-}6)_2][Fp]$in CD_3CN (400 MHz)

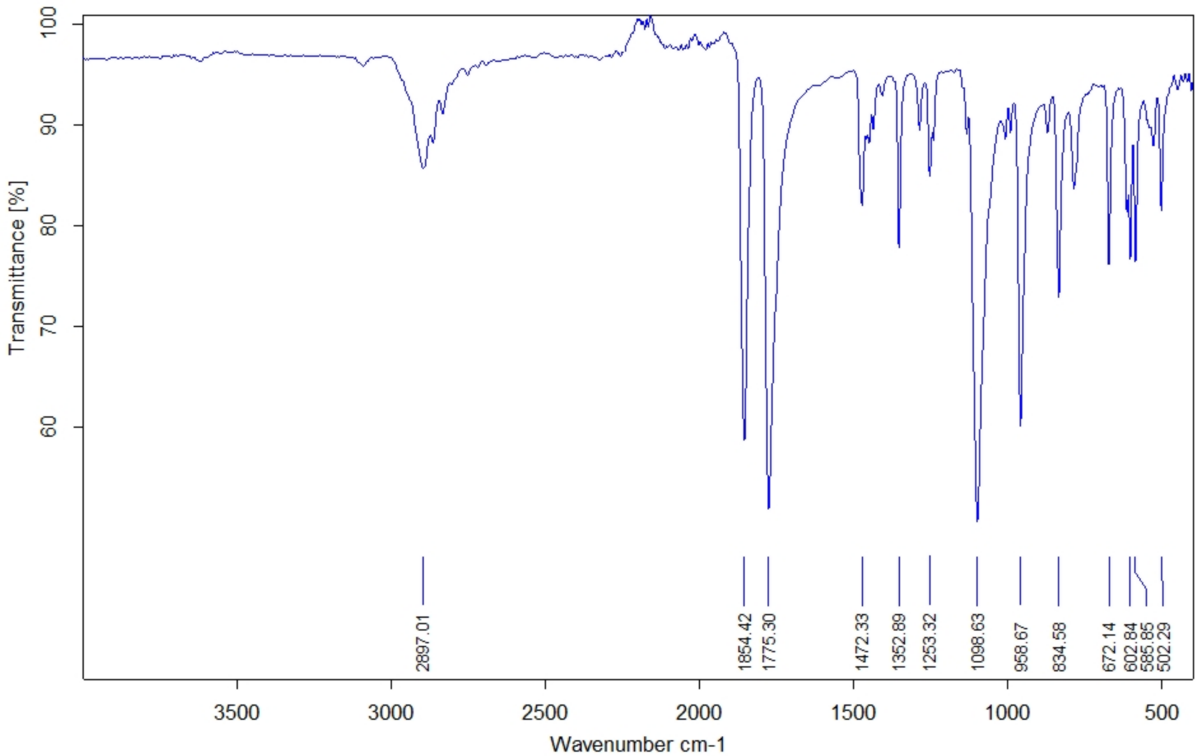

Figure S49: IR Spectrum of $[K(18\text{-crown-}6)_2][Fp]$

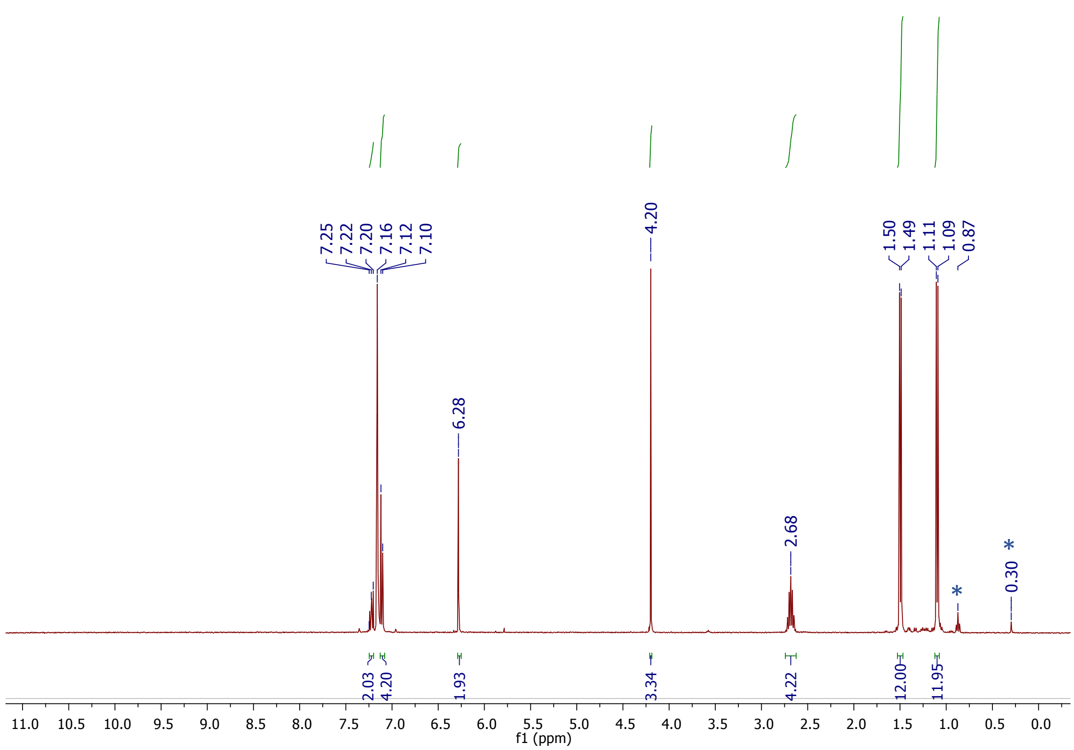

Figure S50: H[1] NMR of (IPr)CuFp in C_6D_6 (400 MHz) *Extra peaks – Grease and Silicon Grease

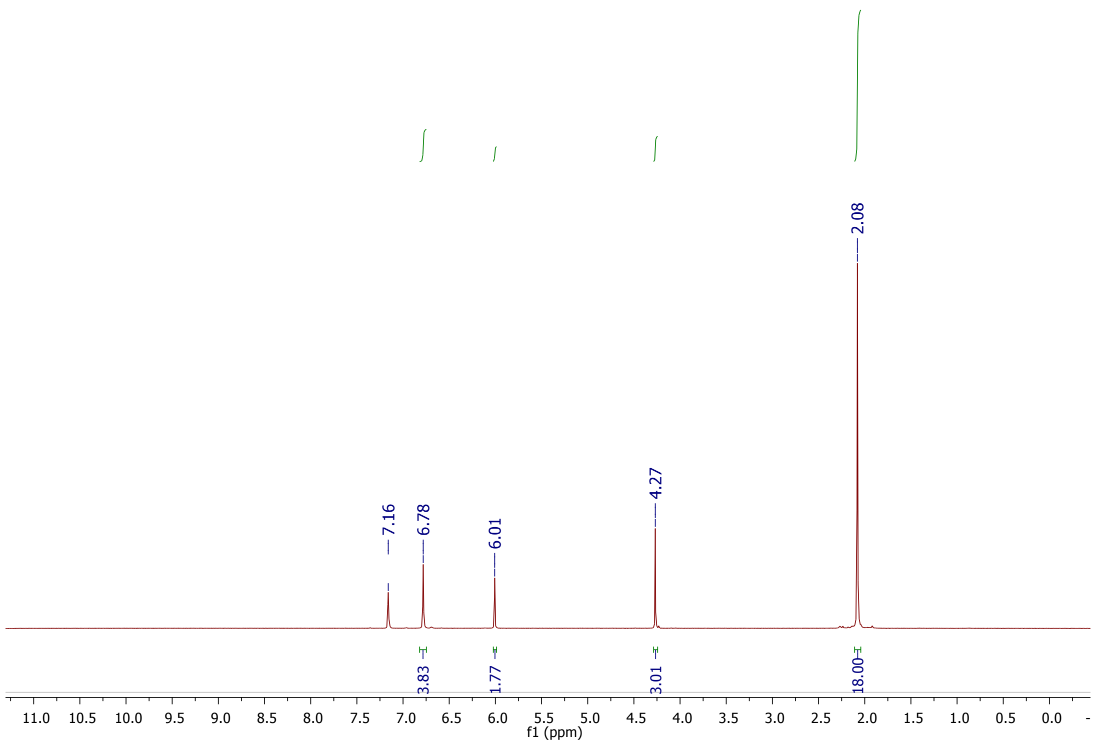

Figure S51: H[1] NMR of (IMes)CuFp in C_6D_6 (400 MHz)

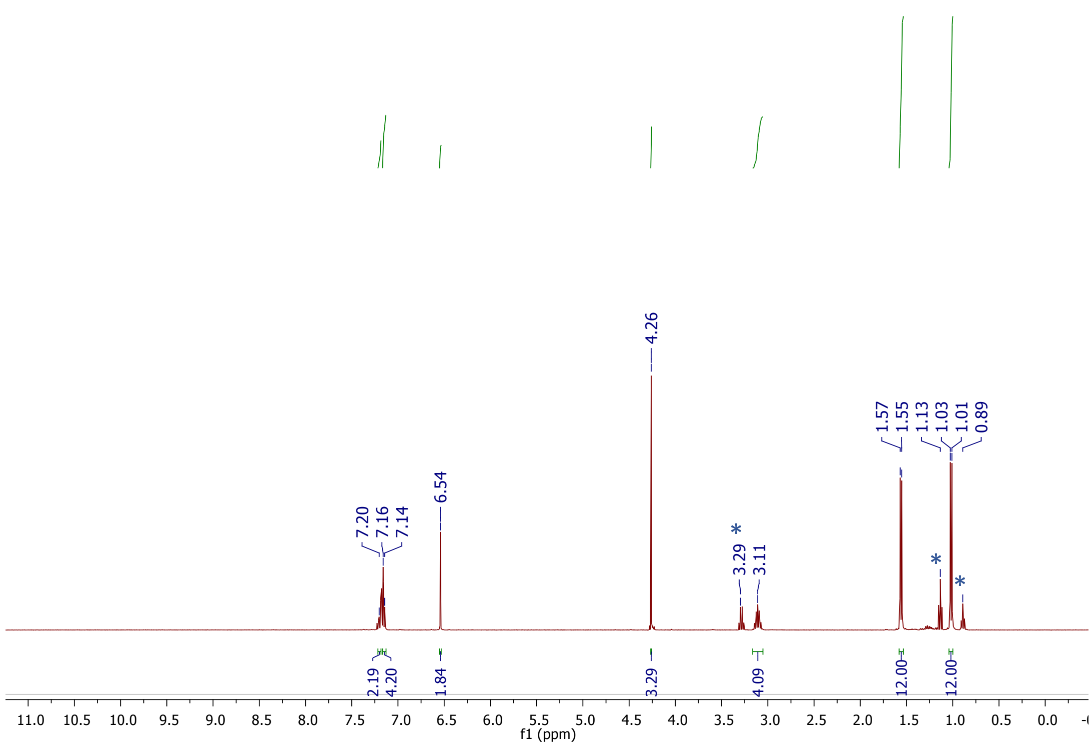

Figure S52 : H[1] NMR of (IPr)ClZnFp in C_6D_6 (400 MHz) *Extra peaks – Diethyl ether and Grease

Table S1. Mössbauer parameters from DFT calculations

Complex	Q (barn)	η	V_{zz} (a.u.)	ΔE_Q^{calcd} (mm/s)	$\rho(0)$ (e/a_0^2)	α(mm/s a_0^2/e)	δ_0 (mm/s)	δ^{calcd} (mm/s)
Fp_2	0.182	0.835	0.782	1.59	1.20	0.164	1903	0.0971
FpI	0.182	-0.872	0.860	1.76	1.35	0.164	1903	0.122
FpMe	0.182	0.684	0.965	1.90	0.537	0.164	1903	-0.0107
(IMe)CuFp	0.0494	0.147	1.53	0.768	0.144	0.108	1250	0.305
(IMe)(Cl)ZnFp	0.0494	0.237	1.41	0.711	1.26	0.108	1250	0.425

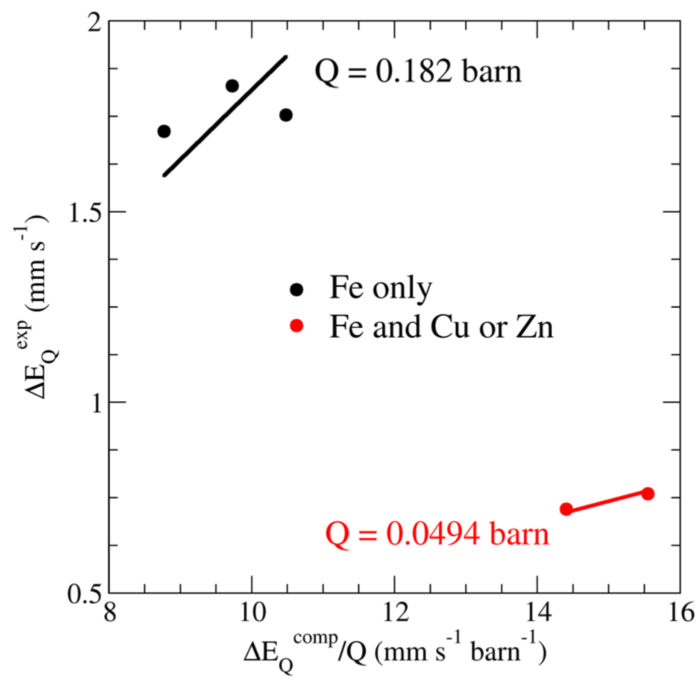

Figure S53 : Fitting used for quadrupole splitting calculations

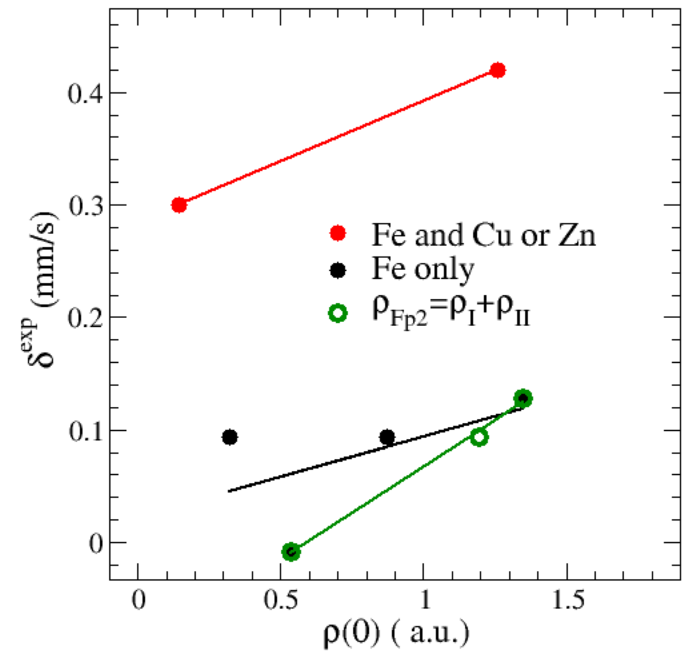

Figure S54 : Fitting used for isomer shift calculations

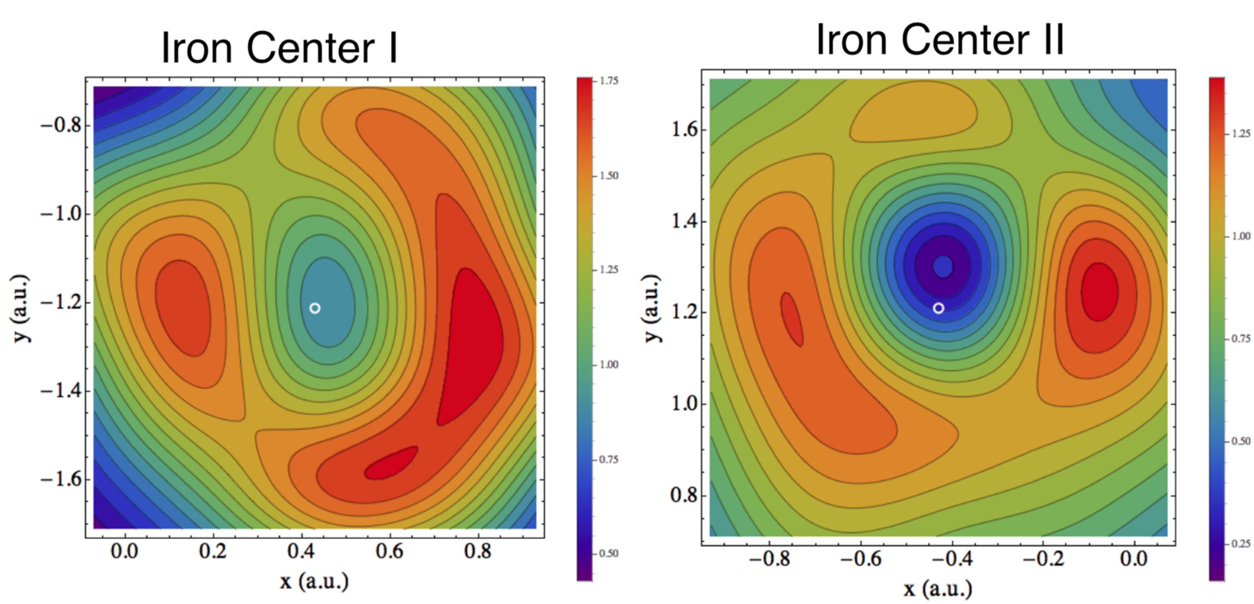

Figure S55 : Calculated electron density plots for the two Fe centers in Fp_2

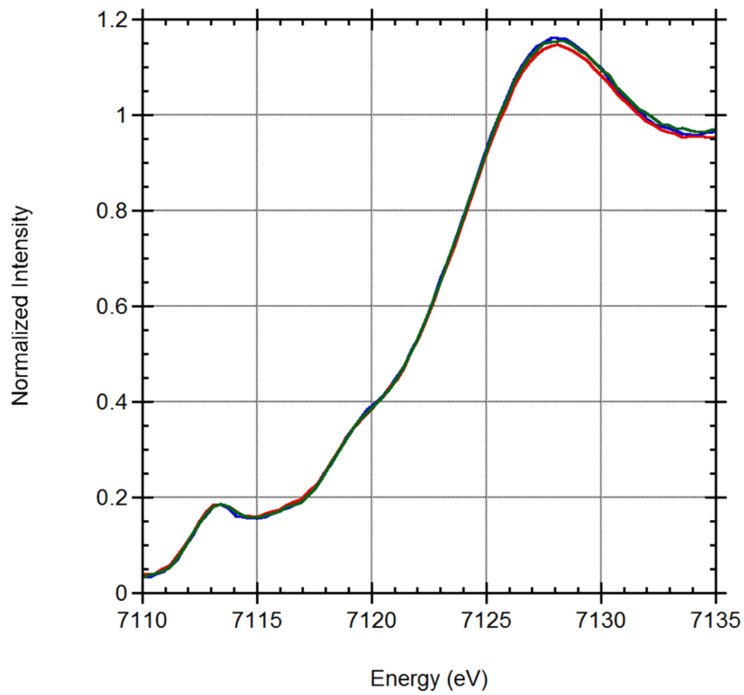

Figure S56 : Monitoring radiation damage : Fe K-edge spectra for (IPr)CuFp – scan 1 (blue) scan 2 (red) and scan 3 (green)

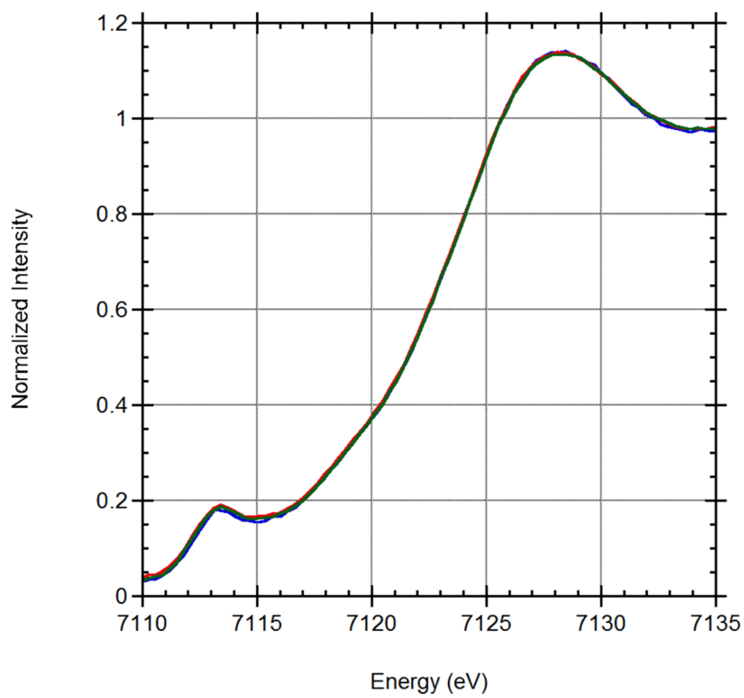

Figure S57 : Monitoring radiation damage : Fe K-edge spectra for (IMes)CuFp – scan 1 (blue) scan 2 (red) and scan 3 (green)

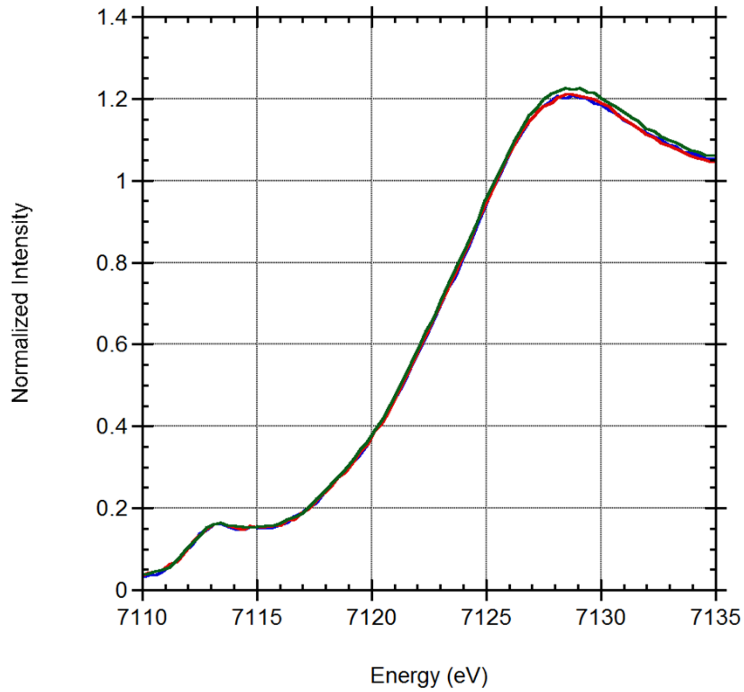

Figure S58 : Monitoring radiation damage : Fe K-edge spectra for (IPr)(Cl)ZnFp – scan 1 (blue) scan 2 (red) and scan 3 (green)

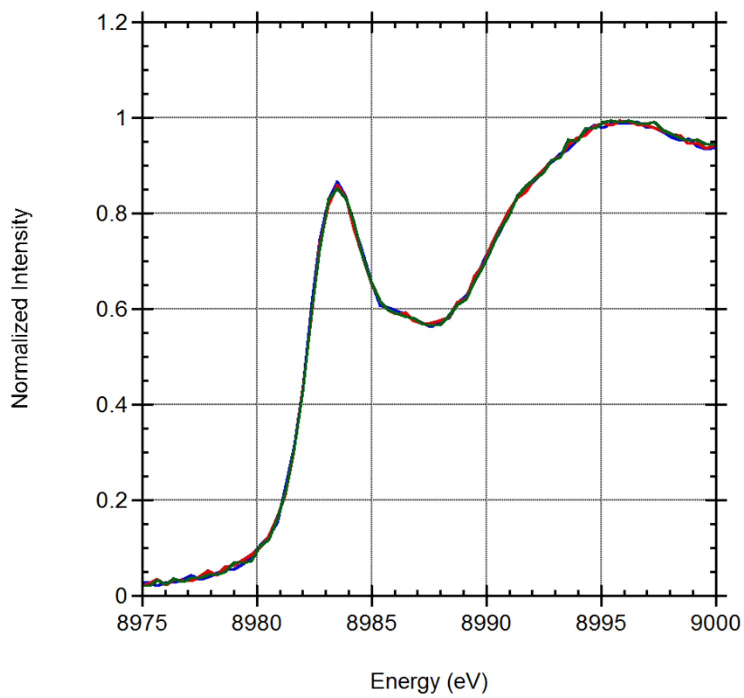

Figure S59: Monitoring radiation damage : Cu K-edge spectra for (IPr)CuFp – scan 1 (blue) scan 2 (red) and scan 3 (green)

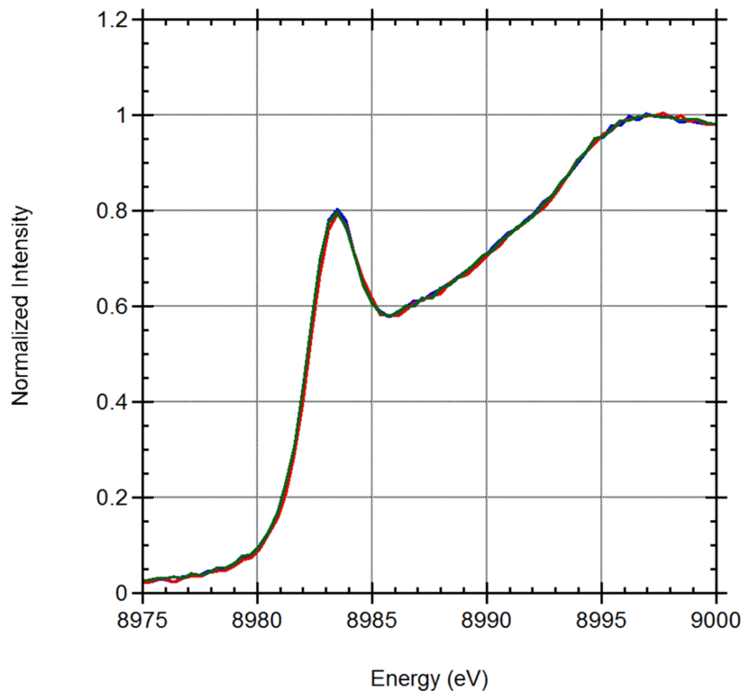

Figure S60: Monitoring radiation damage : Cu K-edge spectra for (IMes)CuFp – scan 1 (blue) scan 2 (red) and scan 3 (green)

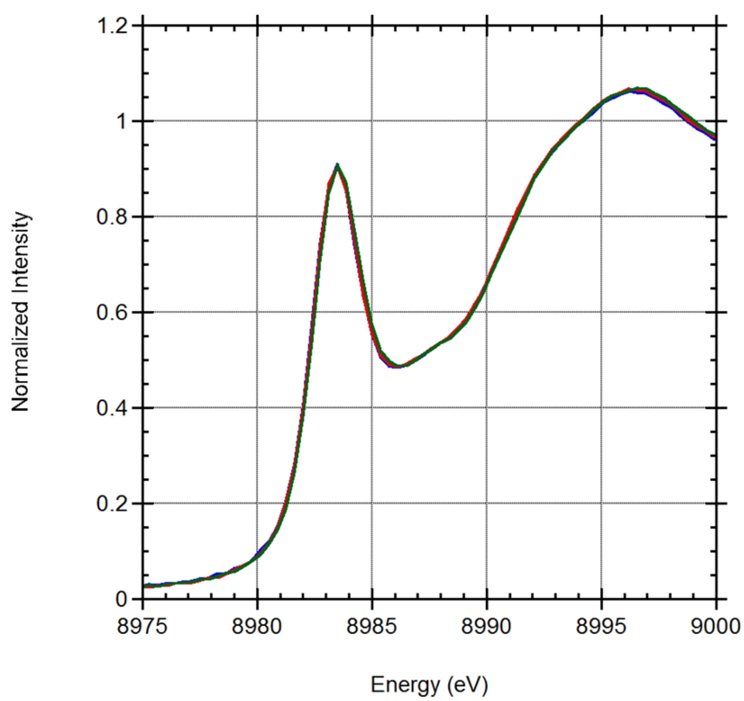

Figure S61: Monitoring radiation damage : Cu K-edge spectra for (IPr)CuMp – scan 1 (blue) scan 2 (red) and scan 3 (green)

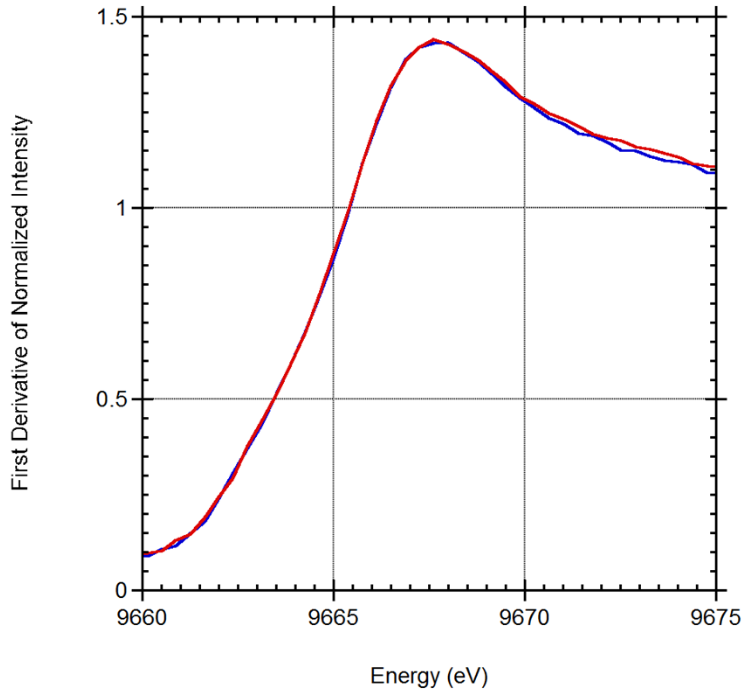

Figure S62: Monitoring radiation damage : Zn K-edge spectrum for (IPr)(Cl)ZnFp – scan 1 (blue) scan 2 (red) and scan 3 (green)

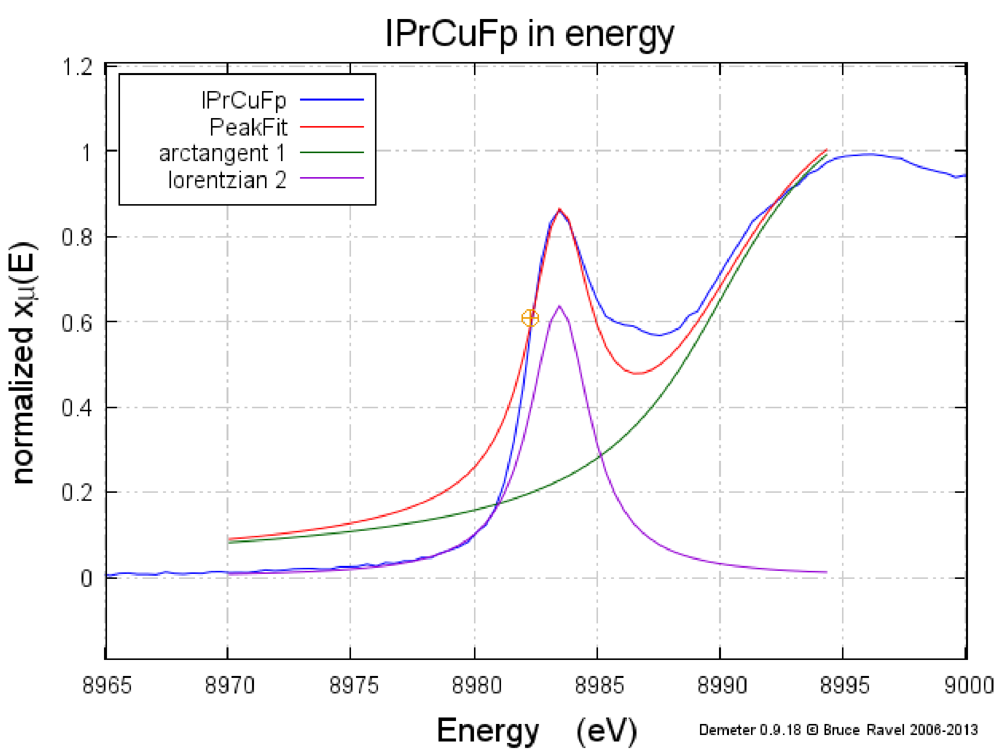

Figure S63: Deconvoluted Cu K-edge spectrum for (IPr)CuFp

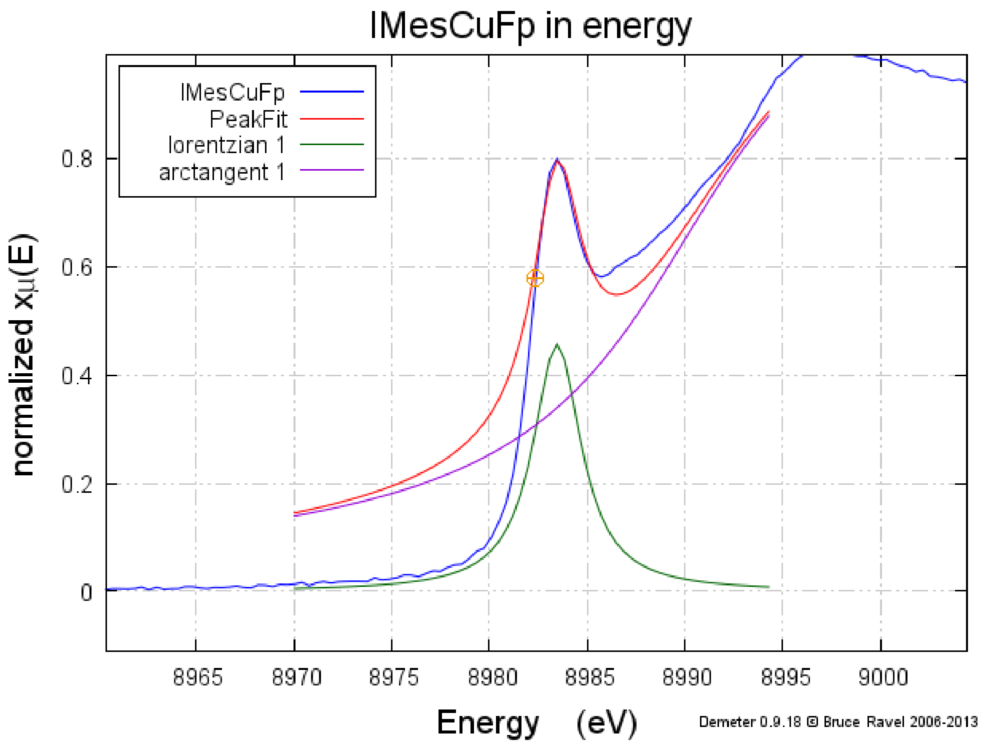

Figure S64: Deconvoluted Cu K-edge spectrum for (IMes)CuFp

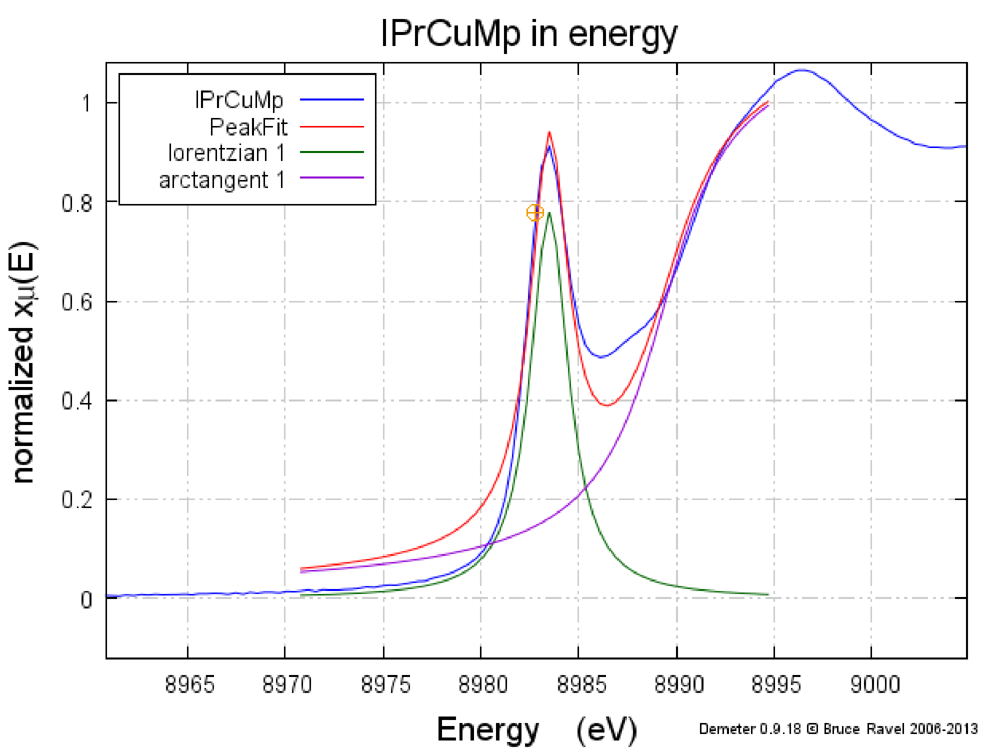

Figure S65: Deconvoluted Cu K-edge spectrum for (IPr)CuMp

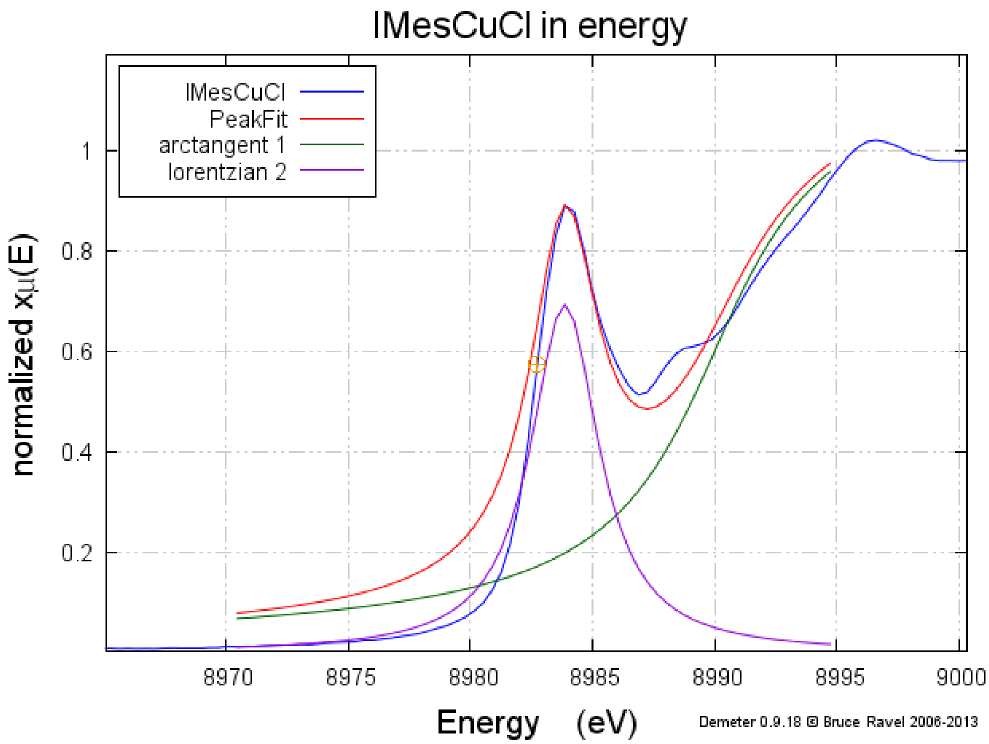

Figure S66: Deconvoluted Cu K-edge spectrum for (IMes)CuCl

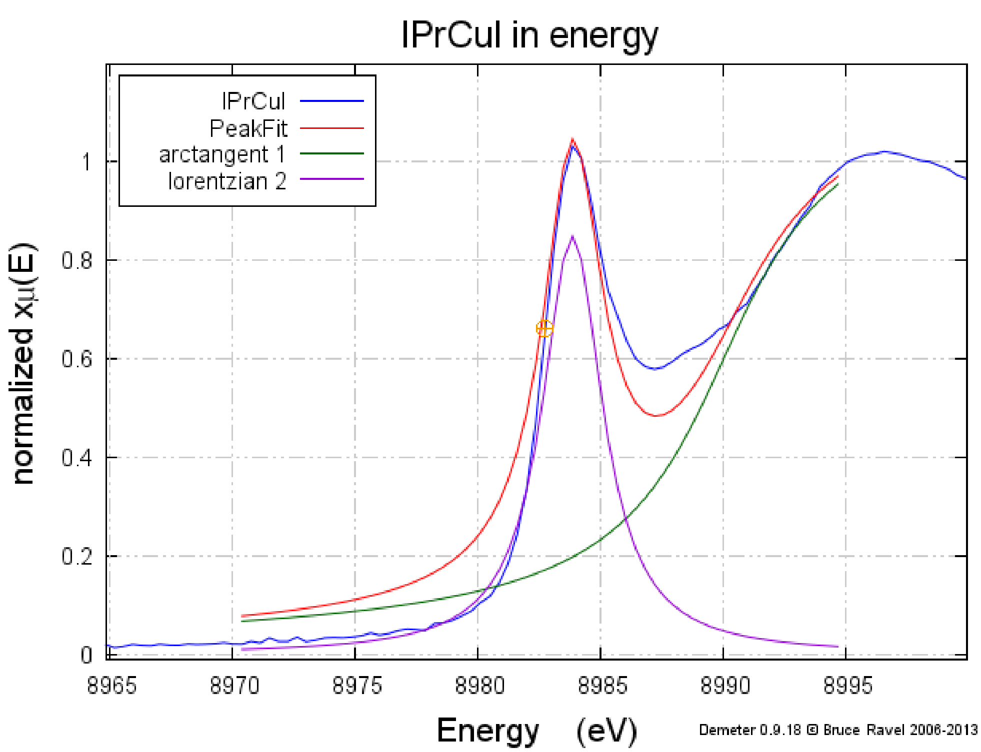

Figure S67: Deconvoluted Cu K-edge spectrum for (IPr)CuI

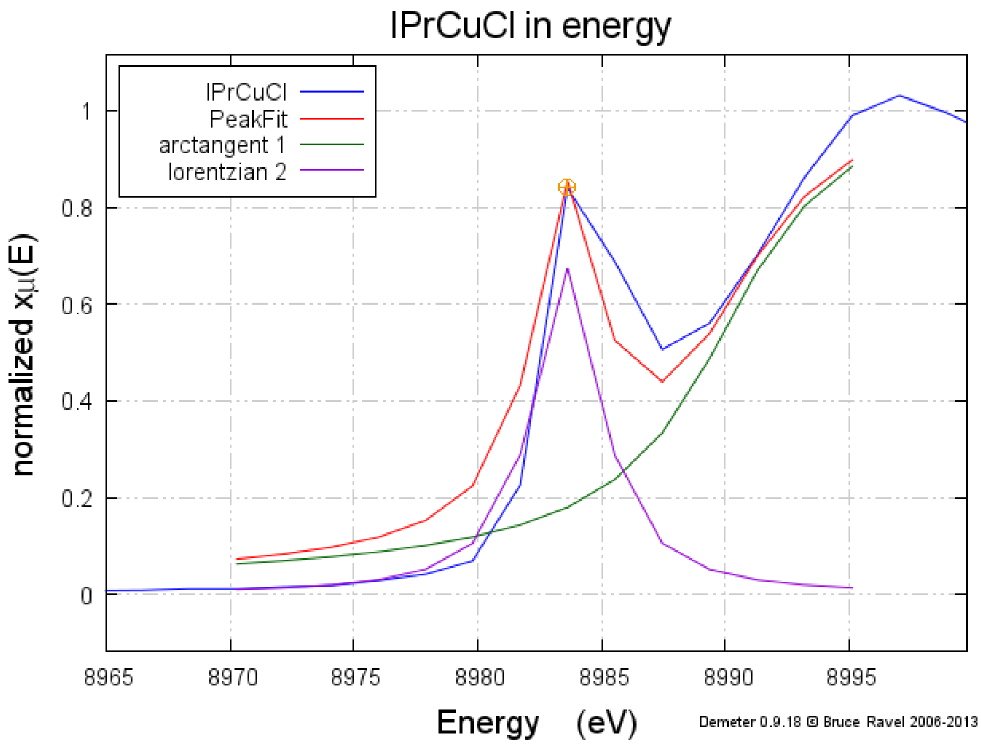

Figure S68: Deconvoluted Cu K-edge spectrum for (IPr)CuCl

Table S2: Deconvolution parameters used for XAS spectra analysis using Athena software[1]

Complex	Fit range	Arctangent			Lorentzian			
		Height	Center	Width	Height	E0	σ	γ
(IPr)CuFp	(-12)-12	1.30	8990.0	4.0	3.00	8983.48	3.0	0.5
(IMes)CuFp	(-12)-12	1.30	8990.0	7.0	2.15	8983.46	3.0	0.5
(IPr)CuMp	(-12)-12	1.17	8989.3	2.6	1.17	8983.50	2.4	0.5
(IMes)CuCl	(-12)-12	1.20	8990.0	3.5	3.70	8983.86	3.4	0.5
(IPr)CuI	(-12)-12	1.20	8990.0	3.5	4.00	8983.84	3.0	0.5
(IPr)CuCl	(-12)-12	1.10	8990.0	3.6	3.50	8983.62	3.3	0.5

[1] B. Ravel, M. Newville, *J. Synchr. Radn*. 2005, **12**, 537-541.

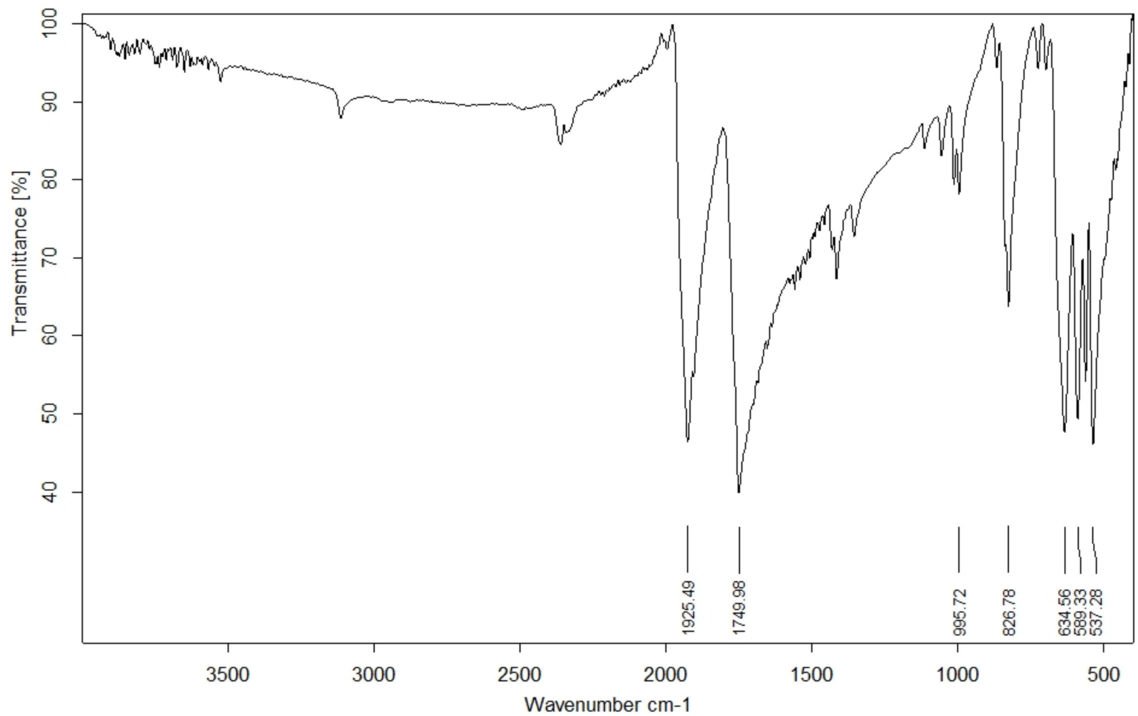

Figure S69: IR Spectrum of Fp_2

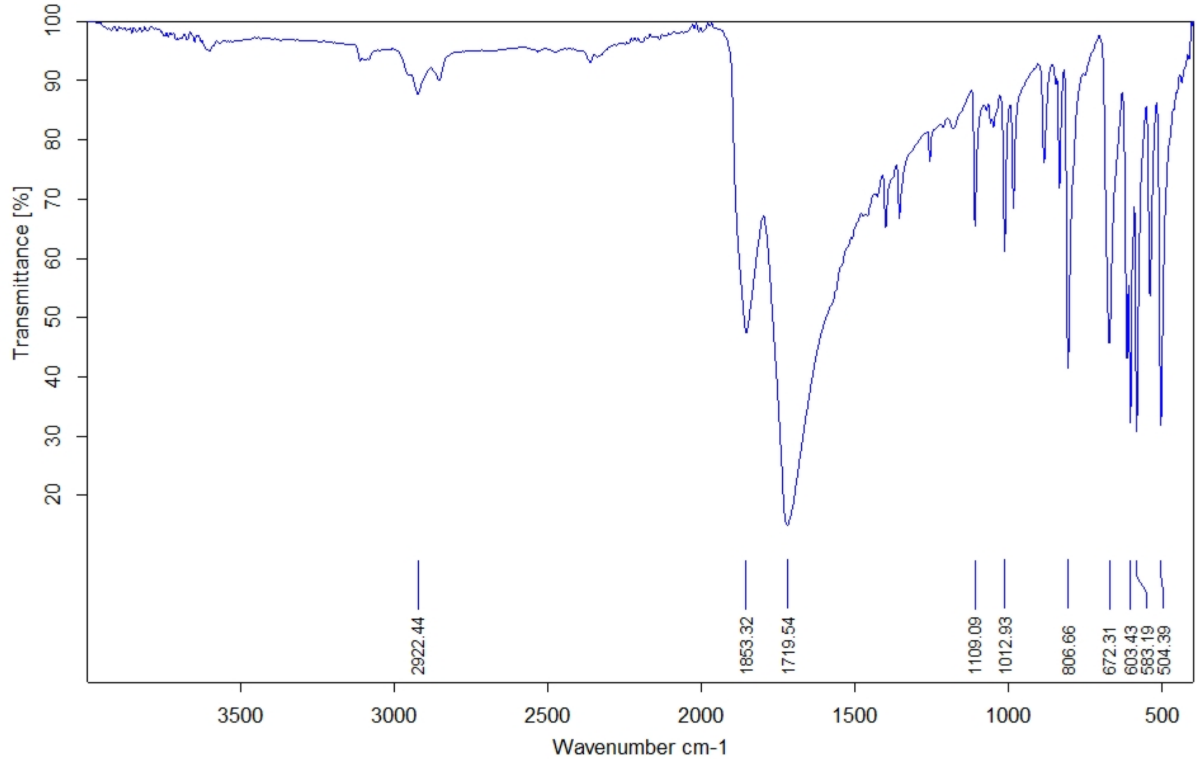

Figure S70: IR Spectrum of K^+Fp^-